DOI: 10.26599/FSHW.2026.9250930

Contents lists available at SciOpen

Food Science and Human Wellness

journal homepage: https://www.sciopen.com/journal/2097-0765

China Food Publishing Co.

Beef tripe-derived peptides ameliorate ulcerative colitis in mice via the MAPK signaling pathway and modulating disorder of gut metabolism

Xuelian Sun[1], Zhifei He[1,2,3], Li Yang[1], Hongjun Li[1,2,3] *

[1.] College of Food Science, Southwest University, No.2 Tiansheng Road, Beibei District, Chongqing 400715, China

[2.] Chongqing Key Laboratory of Special Food Co-Built by Sichuan and Chongqing, No.2 Tiansheng Road, Beibei District, Chongqing 400715, China

[3.] Chongqing Engineering Research Center of Regional Food, No.2 Tiansheng Road, Beibei District, Chongqing 400715, China

ABSTRACT: Beef tripe is rich in high-quality protein, and its enzymatically hydrolyzed peptides exhibit diverse physiological activities. This study investigated their therapeutic potential against dextran sulfate sodium-induced colitis in mice, focusing on three peptides derived from beef tripe (NLPLPPPPPPR, GLGPPSPPAPPR, and HSLPPGPY). Results demonstrated that these peptides alleviated ulcerative colitis symptoms, including reduced weight loss, lower inflammation markers (disease activity index scores, rectal bleeding), improved mental status, and repaired colonic mucosal damage. They also decreased intestinal inflammation, reduced immune cell infiltration (macrophages, neutrophils), and strengthened intestinal barrier function. Mechanistically, peptides inhibited the mitogen-activated protein kinase (MAPK) pathway (JNK, TLR4, p38, ERK phosphorylation), suppressing inflammation. Metabolomic analysis revealed 55 restored gut metabolites critical to anti-inflammatory effects. Overall, beef tripe peptides effectively alleviated colitis by blocking MAPK signaling, restoring gut metabolism, and reducing inflammation, offering a potential therapeutic strategy for ulcerative colitis.

Keywords: beef tripe, anti-inflammatory peptide, ulcerative colitis, gut metabolites, MAPK signaling pathway.

1. Introduction

Ulcerative colitis (UC), a major primary subtypes of inflammatory bowel disease (IBD) marked by chronic recurrent gastrointestinal inflammation[1], is characterized by persistent inflammation and high recurrence rates, which significantly degrade patients' quality of life and causing profound physical and psychological impacts[2]. Therefore, how to prevent and control the incidence of UC and reduce the occurrence of related diseases has become the focus of current research and has great significance. Beef tripe comes from a part of bovine stomach, which is a healthy and nutritious meat by-product and a low-calorie food. In addition to its unique taste, beef tripe also has many nutritional effects, including detoxification, weakness enrichment, essence invigoration, and blood nourishment[3]. Beef tripe is a protein-rich ingredient, containing 14.5 g protein per 100 g fresh sample[4]. As a smooth muscle tissue, it primarily consists of collagen (20.1% of total protein) and elastin (1.0%)[5]. Our previous study[6] demonstrated that beef tripe achieves over

***Corresponding author**
983362225@qq.com

Received 16 June 2025
Received in revised from 7 July 2025
Accepted 30 September 2025

70% protein digestibility after gastrointestinal digestion, rendering it an excellent source of bioactive peptides. Its high digestibility facilitates efficient absorption of these peptides into the human body.

The mitogen-activated protein kinase (MAPK) signaling pathway serves as a critical regulator of inflammation, directly controlling the expression of pro-inflammatory cytokine genes such as interleukin 6 (IL-6), IL-1β, and tumor necrosis factor α (TNF-α)[7]. In colitis, intestinal barrier disruption and increased intestinal permeability enable *Helicobacter* to translocate to intestinal epithelial cells. This bacterial translocation stimulates Toll-like receptor 4 (TLR4) signaling, which subsequently activates the MAPK pathway, thereby inducing the production of pro-inflammatory cytokines and chemokines[8]. Previous studies have confirmed that the MAPK signaling pathway is closely associated with the pathogenesis of UC, and its activation promotes the release of inflammatory mediators and cytokines[9]. After TLR connection, recombinant myeloid differentiation factor 88 (MyD88) is recruited to the Toll domain of the receptor to activate the downstream signaling molecules p38 MAPK, c-Jun N-terminal kinases (JNK), and extracellular signal-regulated kinases (ERK), thereby activating the MAPK pathway, and then promoting the production of inflammatory factors[9]. The MAPK pathway has been demonstrated to be upregulated in colitis patients and experimental colitis animal models[10, 11]. Therefore, the anti-inflammatory effects of bioactive peptides can slow the progression of inflammatory disorders by acting as inhibitors targeting the MAPK pathway.

To better evaluate the biological activities of peptides in the body, animal experiments are usually used to carry out such studies. At present, the most commonly used animal model for evaluating the anti-inflammatory activity of foodborne peptides is the dextran sulfate sodium (DSS)-induced IBD mouse model. Hwang et al.[12] isolated the peptide sequence QCQCAVGEGGL from oyster hydrolysate, which has inhibitory effect on DSS-induced colitis in mice. Feng et al.[13] reported that sea cucumber peptides alleviated DSS-induced intestinal inflammation in mice by suppressing pro-inflammatory cytokine production and inhibiting inflammatory factor secretion. Meanwhile, studies have found that the novel peptide PHP1 derived from rice dreg exerts its anti-inflammatory effects by inhibiting the IL-17/MAPK signaling pathway and activating the RAS-ERK signaling pathway[14]. The novel peptide LLEL from sturgeon cartilage blocks the phosphorylation of MAPKs, thereby exerting anti-inflammatory effects[15]. Additionally, silkworm pupa peptides reduce colonic inflammation in mice by suppressing the activation of the MAPK signaling pathway[16].

In our previous studies, we have identified three new anti-inflammatory peptides (NLPLPPPPPPR, GLGPPSPPAPPR, and HSLPPGPY) in beef tripe after gastrointestinal digestion[6] and verified their anti-inflammatory activity *in vitro* through the LPS-induced RAW264.7 macrophage inflammation model. Results demonstrated that these peptides attenuated pro-inflammatory mediators (NO, TNF-α, IL-6) via modulation of the MAPK signaling pathway. However, limited investigations have examined the anti-inflammatory effects of beef tripe peptides *in vivo*. This study sought to evaluate the anti-inflammatory activity of beef tripe peptides in mice with DSS-induced colitis by assessing the protection of colon structure and the secretion of inflammatory factors, while further elucidating the underlying mechanisms. The novelty

of this research lies in exploring the mechanism of action of the novel bioactive peptides from beef tripe in exerting their anti-inflammatory effects *in vivo*. This study will provide a theorical reference for the development and preparation of beef tripe bioactive peptide and its derived functional food or health products.

2. Materials and methods

2.1 Materials and reagents

Three beef tripe peptide sequences, namely NLPLPPPPPPR, GLGPPSPPAPPR, and HSLPPGPY, were synthesized using the solid-phase synthesis method at a purity of > 98% by Shanghai Hongtide Biotechnology Co., Ltd (Shanghai, China). The peptides were stored in the -80 ℃ refrigerator for further analysis. DSS (MW 36000–50000 kDa) was purchased from MP Biomedicals (Solon, OH, USA). IL-1β, IL-6, IL-10, TNF-α, and neutrophil-myeloperoxidase (MPO) enzyme linked immunosorbent assay (ELISA) kits were obtained from Jiangsu Meimian Industrial Co., Ltd (Yancheng, China). The antibodies for ERK, JNK, p38 kinase (p38), β-actin, lymphocyte antigen 6G (Ly6G), and mouse EGF-like module-containing mucin-like hormone receptor-like 1 (F4/80) were procured from Abcam Limited (Cambridge, UK). Hematoxylin staining solution, eosin staining solution, bicinchoninic acid (BCA) protein assay kit, and neutral gum were obtained from Beyotime Biotechnology Co., Ltd (Shanghai, China). Enhanced chemiluminescence (ECL) kit was obtained from Biosharp Life Sciences Co., Ltd (Hefei, China).

2.2 Animals and experimental design

The DSS-induced UC mouse model was established as described by Hu et al.[17] with slight modification. For this study, 50 male C57BL/6J mice (6 weeks) Specific Pathogen Free (SPF grade) were purchased from Laboratory Animal Research Center of Hubei Province (Wuhan, China; Animal production License No.: SCXK (E) 2020-0018). Experimental procedures were approved by the Laboratory Animal Ethics Review Committee of Southwest University (Certificate No. IACUC-20250304-33) and conducted in accordance with internationally recognized ethical guidelines and standards. Animals were maintained in a SPF environment with independent ventilation, under a 12-h light/12-h dark cycle, 55% ± 5 humidity, and had free access to food and water. Mice were housed in groups of 3–4 per cage after a one-week acclimation period. The cages were disinfected weekly and bedding replaced twice a week.

According to the pre-experiment results, 1200 mg/kg body weight (BW) of each beef tripe peptide was selected for the animal experiment. The experimental design is illustrated in Fig. 1A. Mice were randomly assigned to 5 groups (each n = 10): normal group (NC), model group (MC), NLPLPPPPPPR group (NL), GLGPPSPPAPPR group (GL), and HSLPPGPY group (HS). All groups, except the NC, were treated with 3% (w/v) DSS to induce colonic inflammation for ten consecutive days. NL, GL, and HS received their respective drugs via daily oral gavage over the same period. Meanwhile, the NC was given water daily at the same dose as the treatment groups. Each group of mice was treated at a fixed time every day.

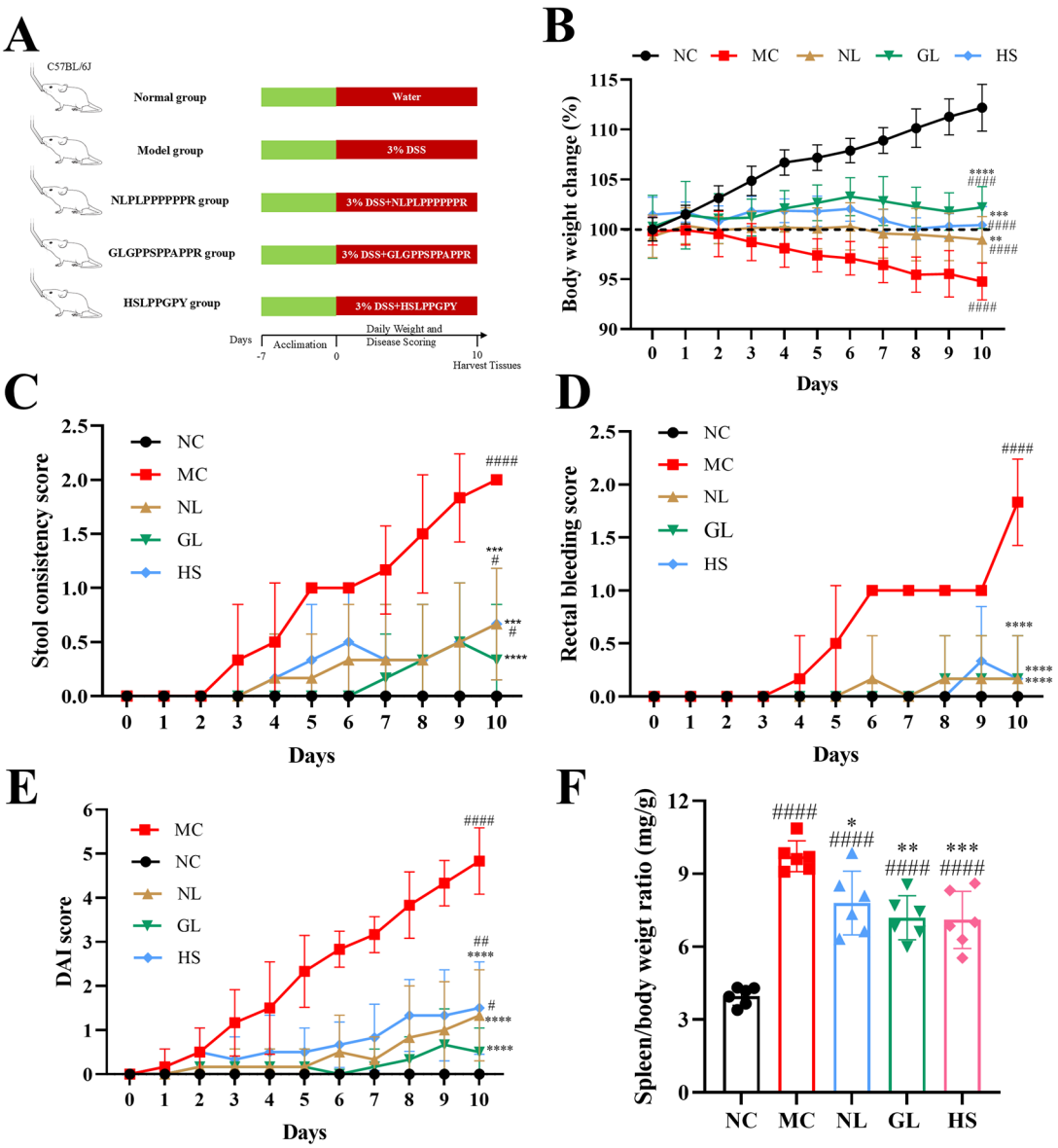

Fig. 1. Effects of beef tripe peptides treatment on phenotypic symptoms in DSS-induced UC mice. A. Animal experimental design. B. Daily body weight changes in mice. C. Daily stool consistency in mice. D. Daily rectal bleeding in mice. E. Daily evaluation of DAI score in mice. F. Spleen index in mice. Note: $^{\#}P < 0.05$, $^{\#}P < 0.01$, $^{\#\#\#\#}P < 0.0001$ vs. NC; $^{*}P < 0.05$, $^{**}P < 0.01$, $^{***}P < 0.001$, $^{****}P < 0.0001$ vs. MC.

2.3 Disease activity index (DAI) assessment

In the entire process of the experiment, body weights, stool consistency, and blood stool of mice were monitored every day. The DAI was calculated based on the method of Liu et al.[18] using the parameters presented in Table S1.

2.4 Anatomy and body tissue collection of mice

At experiment termination, the mice were euthanized and dissected, with tissue samples collected for analysis. The serum samples were obtained following centrifugation at 3000 r/min for 15 min, and then stored at -80 °C. The colon and rectum of mice were separated, the colonic tissue traits and intestinal contents were observed, and the colon length was measured. The colonic tissues were washed gently with phosphate buffer and dried with filter paper. The colonic tissues were weighed, and the data were recorded. After that, each

colonic tissue was cut into several segments. Some parts were fixed with 4% paraformaldehyde, and the other parts were quickly frozen with liquid nitrogen and stored at -80 ℃ for further analysis.

2.5 Hematoxylin and eosin (H&E) staining

The colonic tissues underwent sequential dehydration in ethanol solutions followed by ethanol xylene clearing, and subsequently embedded in paraffin. After that, they were sliced into 3 μm pieces and baked. These tissue slices were stained with hematoxylin, then dyed with 0.5% eosin, and sealed with neutral gum. The colonic structures were observed and photographed under a microscope (Olympus, Tokyo, Japan). Histological scores were performed for colitis and the depth of crypts was measured.

2.6 Immunohistochemical analysis

The colonic tissue segments were dehydrated using gradient ethanol, transparent with ethanol xylene and xylene, and embedded in paraffin. Then they were made into 4 μm slices and baked in an oven at 65 ℃ for 60 min. After the repair in the microwave oven, the slices were put into phosphate buffer solution (PBS), incubated at 4 ℃ overnight with drops of primary antibody (Ly6G and F4/80), washed with PBS, added with secondary antibody for incubation at 37 ℃ for 20 min in the dark environment. Afterwards, they were washed with PBS, dripped with diaminobenzidine (DAB) dye solution for color development, added with hematoxylin for counterstain, dehydrated with gradient ethanol, used xylene for transparency, and sealed with neutral gum on slides. At last, the slides were observed and photographed using a microscope (Olympus, Tokyo, Japan). Images were collected and analyzed using Image-pro plus 6.0 (Media Cybernetics, Inc., Rockville, MD, USA), and the average optical densities of Ly6G and F4/80 positive cells were calculated.

2.7 ELISA analysis

Serum levels of IL-1β, IL-6, IL-10, TNF-α, and MPO activity were detected using the corresponding ELISA kits according to the instructions in the manufacturer's manual.

2.8 RNA extraction and quantitative real-time PCR (qRT-PCR) analysis

Total RNA was extracted from standardized distal colon sections using the TriQuick total RNA extraction kit (Solarbio Co., Ltd., Beijing, China) following the manufacturer's protocol. Subsequently, cDNA was synthesized using a gDNA Eraser Prime Script RT Kit (Takara Bio, Inc., Shiga, Japan). Then, qRT-PCR analysis was performed using Thermo Fisher Scientific QuantStudio 1 Real-Time PCR System (Waltham, MA, USA). The primer sequences utilized in this study are listed in Table 1.

Table 1 Mice primer sequences in qRT-PCR assays.

Genes	Forward	Reverse
actin	AGGGAAATCGTGCGTGACAT	CGTTGCCAATAGTGATGACC
ZO-1	TGGCAAGCGATCATACCCAGAG	CTGCCTGAAGTCATCCACACTC
Occludin	GGACTGTGGATGTCCTGCGTTT	GCCAATTACCATCAAGGCTCGG
Claudin-1	GCCCACCTCACAAGCAGTAT	GTCATAGCCAGGGGCAAACT
Muc2	GTTGGTACGGTGCCCTGAAAGA	GCTGACAGGTAGGACAGACGAT
Reg3b	TGGCTCCTACTGCTATGCCTTG	CGCTATTGAGCACAGATACGAGG
Reg3g	CGTGCCTATGGCTCCTATTGCT	TTCAGCGCCACTGAGCACAGAC

2.9 Western blot detection

Mouse colonic tissues were lysed in radio immunoprecipitation assay (RIPA) buffer supplemented with phenylmethylsulfonyl fluoride (PMSF) to extract proteins. Protein concentration was measured via BCA assay using bovine serum albumin (BSA) as the standard. Based on the measured concentration, the loading volume was calculated, mixed with 5× sodium dodecyl sulphate polyacrylamide gel electrophoresis (SDS-PAGE) loading buffer, and subjected to heat denaturation (95 ℃ for 10 min), followed by storage at -80 ℃. Proteins were separated by SDS-PAGE and then transferred to polyvinylidene difluoride (PVDF) membranes. After blocking with 5% BSA, the membranes were incubated with specific primary antibodies at 4 ℃ overnight, followed by three washing cycles. Subsequently, they were incubated with secondary antibodies at room temperature (25 ℃) for 1 h and washed three additional times. Protein bands were visualized using an ECL kit, and grayscale intensities were quantified via Image J software (Rawak Software Inc., Stuttgart, Germany).

2.10 Metabolomic analysis

A 50 mg sample of cecum contents was mixed with 400 μL extraction solvent (methanol: water, 4:1, v/v), supplemented with 0.02 mg/mL L-2-chlorophenylalanine (internal standard). The mixture underwent cryogenic homogenization (cryogenic homogenizer, -10 ℃, 50 Hz, 6 min) followed by ultrasonication at low temperature (5 ℃, 40 kHz, 30 min). After centrifugation at 4 ℃ and 13000 × *g* for 15 min, the supernatant was collected for ultra high-performance liquid chromatography-tandem mass spectrometry (UHPLC-MS/MS) analysis. Mass spectrometric analysis was performed using UHPLC-Q Exactive HF-X system (Thermo Fisher Scientific, California, USA) in positive and negative ion scanning modes, with an ACQUITY HSS T3 column (100 mm × 2.1 mm i.d., 1.8 μm; Waters Corporation, Milford, USA) for separation. Subsequent LC-MS/MS data processing was carried out via Progenesis QI (Waters Corporation, Milford, USA). Concurrently, the metabolites were identified using the Human Metabolome Database (HMDB, http://www.hmdb.ca/), Metlin (https://metlin.scripps.edu/), and the Majorbio Database (MJDB) of Majorbio Biotechnology Co., Ltd. (Shanghai, China). Significant different metabolites were selected based on variable importance in projection (VIP) values from orthogonal partial least squares-discriminant analysis (OPLS-DA) model and the p-values generated by student's t-test, with criteria set at VIP > 1 and $P < 0.05$.

2.11 Statistical analysis

Data were expressed as mean ± standard deviation (SD). Experiment data were analyzed using One-way ANOVA (SPSS Statistics 25.0, IBM, Inc., USA), followed by post-hoc analysis using Duncan's multiple range test. Graphs were created using GraphPad Prism (version 9, GraphPad Software, USA) and Origin 2022 (OriginLab, USA).

3. Results and discussion

3.1 Effect of beef tripe peptides on general symptoms in DSS-induced colitis mice

UC was induced in C57BL/6J mice via oral administration of 3% DSS solution. Following a 7-day adaptation period, the mice were randomly divided into groups. The MC was administered DSS-supplemented drinking water for 10 consecutive days to induce a UC model, after which the effects of the peptides NLPLPPPPPPR, GLGPPSPPAPPR, and HSLPPGPY were evaluated in these mice. Oral gavage is suitable for studies simulating human medication or local intestinal effects, but it is limited by bioavailability and dosage constraints[19]. In contrast, injection routes (intraperitoneal, intramuscular, intravenous) offer higher efficacy and controllability but involve greater invasiveness[20]. Given the study's objective to investigate the effects of beef tripe peptides on the mouse intestinal tract after digestion and validate their potential as dietary supplements for treating colitis, oral gavage was chosen as the most suitable method.

Body weight was tracked throughout the experimental period (Fig. 1B). Mice in NC exhibited a gradual increase in body weight over the entire duration. Compared with NC, the mice in MC demonstrated a decline in body weight starting from the second day of DSS administration, showing the greatest body weight loss of day 10 (94.8%) of initial value. Such a decrease was significant compared with NC ($P < 0.0001$), indicating successful UC modeling. As the experiment progressed, MC and NL displayed an overall downward trend in body weight, while GL and HS showed an overall upward trend in body weight. Notably, administration of beef tripe peptides significantly attenuated the DSS-induced weight loss compared with MC ($P < 0.01$). In addition, the mental status, rectal bleeding, and stool consistency of mice were monitored throughout the experiment. Mice in NC maintained a vibrant and active demeanor, with smooth, glossy fur and formed pellets consistent with normal stool morphology. Compared with NC, mice in MC exhibited signs of lethargy, mild diarrhea, soft stools, and positive fecal occult blood tests by day 4 post-DSS administration (Fig. 1C&D). By day 9, mice with UC displayed severe lethargy, hunched posture, and varying degrees of watery hematochezia and rectal bleeding. Compared with MC, the administration of beef tripe peptides significantly alleviated the aforementioned DSS-induced symptoms, as evidenced by significant reductions in stool consistency scores and fecal bleeding scores ($P < 0.001$) on day 10. The DAI score serves as an indicator of UC severity, with results presented in Fig. 1E. The DAI score in MC rose sharply throughout the experimental period. On day 10, DAI in MC was significantly higher than that in NC ($P < 0.0001$). For all beef tripe peptide groups, DAI began to decline significantly on day 3 compared with MC. At the end of the experiment, on day 10, DAI scores in beef tripe peptide groups were significantly lower than that in MC ($P < 0.0001$), indicating that UC progression was substantially suppressed. The spleen, being the most crucial immune organ in the body, exhibits splenomegaly (enlargement) as a phenotypic indicator of systemic inflammation[21]. As shown in Fig. 1F, compared with NC, the spleens of DSS-induced colitis mice were extremely enlarged ($P < 0.0001$), indicating splenic damage in these mice. Notably, treatment with beef tripe peptides significantly reduced the spleen index ($P < 0.05$).

Natural products, particularly bioactive peptides, hold a significant promise as therapeutic candidates for UC treatment development. Chen et al.[22] showed that a novel millet gliadin peptide (VSAAAA) ameliorated DSS-induced phenotypic symptoms (weight loss, shortened colon length, and increased DAI). Fan et al.[23]

found the amelioration of weight loss, the inhibition of DAI elevation, and improvement of symptoms (such as colon atrophy and shortening) in UC mice treated with a duck liver protein peptide VIESPPEI. In the present study, the results demonstrated that treatment with beef tripe peptides suppressed phenotypic changes in DSS-induced UC mice, reduced mortality rates, and alleviated UC symptoms.

3.2 Effect of beef tripe peptides on colon in DSS-induced colitis mice

Colon shortening is one of the typical symptoms of UC. Therefore, we measured the colon length in mice. As shown in Fig. 2A and B, DSS-induced colitis mice in the MC group exhibited significant colon shortening compared with NC, with colon length reduced from 7.07 cm to 4.88 cm, which is a hallmark feature of UC. However, after treatment with beef tripe peptides, colon length was significantly increased compared with MC ($P < 0.0001$). Specifically, the NL, GL, and HS groups showed recoveries to 6.44 cm (31.97% increase compared with MC), 6.35 cm (30.12%), and 6.27 cm (28.48%), respectively. These findings demonstrated that beef tripe peptides had an ameliorative effect on DSS-induced colon shortening.

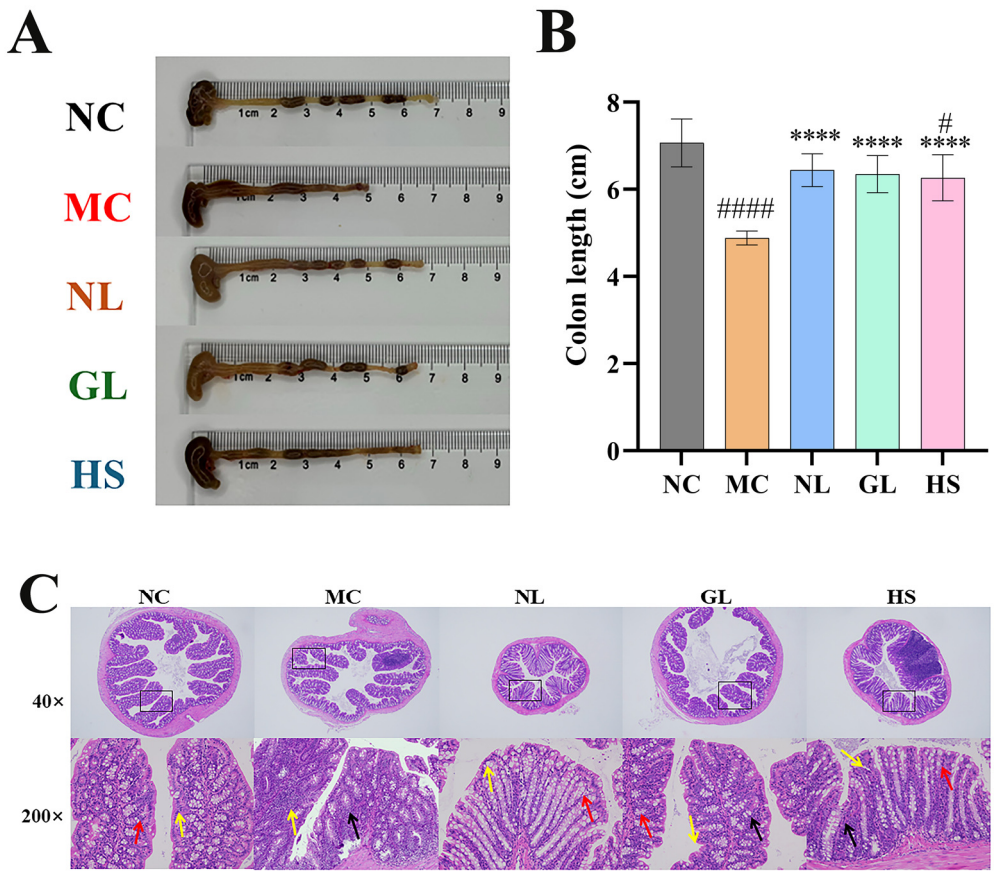

Fig. 2. Changes of colon in DSS-induced colitis mice. A. Representative images of the observed colons. B. The lengths of colons from each group. C. Representative photomicrographs of colonic histology by H&E staining (magnification 40× and 200×). Note: $^{\#}P < 0.05$, $^{\#\#\#\#}P < 0.0001$ vs. NC; $^{****}P < 0.0001$ vs. MC.

To further observe the microarchitecture of intestinal tissue, H&E staining was systematically performed on mouse colonic sections (Fig. 2C). In NC, the overall structure of the colonic tissue appeared essentially normal, with well-organized mucosal epithelial cells and no evidence of epithelial cell shedding or necrosis (the yellow arrow indicates mucosal epithelial cells). In the mucosal layer, the number of goblet cells remained abundant without significant reduction (the red arrow points to goblet cells). No obvious edema or

looseness was observed in the submucosal layer, and there was no marked infiltration of inflammatory cells in the tissue. MC showed that the colonic tissue exhibited abnormal overall architecture, with extensive degeneration and necrosis of mucosal epithelial cells. In necrotic areas, nuclei showed pyknosis and lysis (the yellow arrow indicates). Additionally, marked infiltration of inflammatory cells was observed throughout the tissue, with inflammatory cells penetrating through the entire tissue layer (indicated by the black arrow). NL showed that the colonic tissue exhibited an essentially normal overall structure, with well-arranged mucosal epithelial cells and no signs of epithelial cell sloughing or necrosis (the yellow arrow denotes mucosal epithelial cells). In the mucosal layer, goblet cells were abundant without significant reduction (the red arrow indicates goblet cells). The submucosal layer showed no evident edema or structural loosening, and no substantial inflammatory cell infiltration was observed in the tissue. GL and HS showed that the colonic tissue demonstrated mild overall structural abnormalities, with mucosal epithelial cells arranged in a relatively orderly pattern (the yellow arrow denotes mucosal epithelial cells). No signs of epithelial cell sloughing or necrosis were observed. In the mucosal layer, goblet cells were abundant, showing no marked reduction (the red arrow indicates goblet cells). The submucosal layer exhibited no significant edema or structural loosening. However, minimal inflammatory cell infiltration was noted in the tissue (the black arrow highlights the infiltrating cells, as shown in the figure).

The intestinal epithelium and mucus layer collectively form a vital physical barrier, acting a critical defense mechanism that prevents toxic substances from entering the intestinal tract and thereby maintaining intestinal homeostasis[24]. Upon activation, goblet cells secrete mucus continuously, forming a protective barrier with the intestinal tract. A decline in goblet cell mucus production is recognized as a key pathological hallmark of colitis progression[25]. In this study, we observed a significant reduction in colonic goblet cells following DSS induction, whereas the interventions of beef tripe peptides effectively preserved the number of goblet cells. These findings indicated that protective effects of beef tripe peptides on colonic tissues.

3.3 Effect of beef tripe peptides on MPO activity

MPO, a cationic protein residing in neutrophils and monocytes[26], induces epithelial injury via the generation of reactive oxygen species (ROS). Its activity exhibits a direct proportional relationship with neutrophil concentration in inflamed tissues[27]. Assessment of MPO activity serves as a reliable biomarker for evaluating inflammation severity and neutrophil infiltration in murine models. As shown in Fig. 3A, the mice in MC exhibited an extremely significant elevation in serum MPO level compared to NC ($P < 0.0001$), which were 270.32 pg/mL and 119.38 pg/mL, respectively. Elevated MPO levels suggest neutrophil infiltration and dysregulation of the inflammatory cascade, a phenomenon confirmed in animal models and also observed in patients with IBD[28]. Therefore, this phenomenon indicated potential neutrophil infiltration in the colonic mucosa of DSS-induced colitis. Treatment with three beef tripe peptides (1200 mg/kg BW) significantly reduced the MPO levels to 141.62 pg/mL (NL, $P < 0.0001$), 227.78 pg/mL (GL, $P < 0.01$), and 179.30 pg/mL (HS, $P < 0.0001$), respectively, compared to MC. These results suggested that beef tripe peptides might suppress neutrophil infiltration, thereby downregulating MPO-driven inflammation *in vivo*. It has been

reported that bioactive peptides could suppress vascular permeability, reduce inflammatory cell infiltration, and mitigate tissue edema[16].

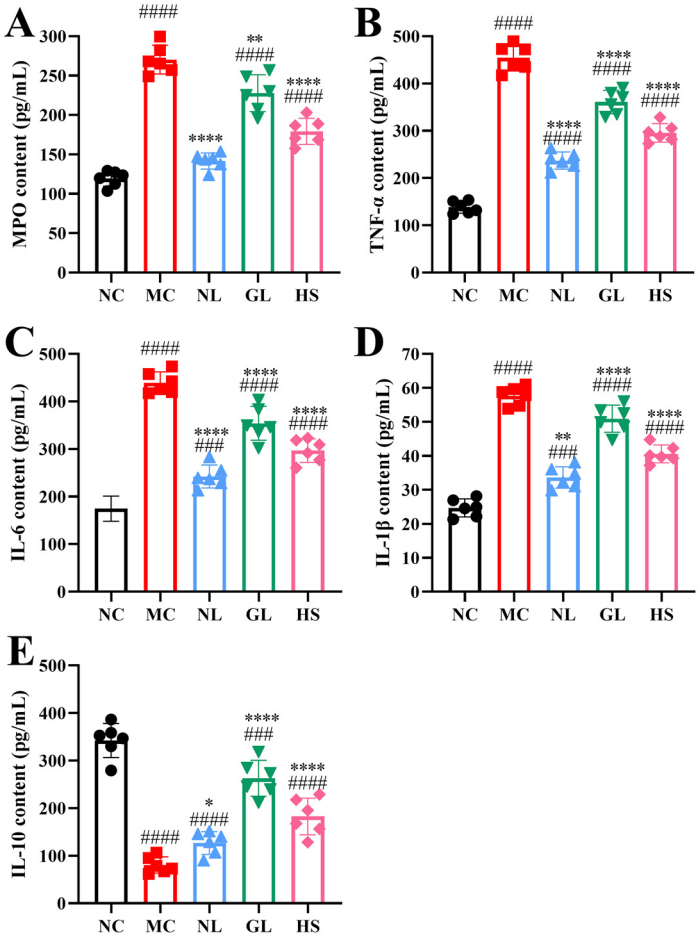

Fig. 3. Effects of beef tripe peptides on the content of related enzymes and

3.4 Effect of beef tripe peptides on inflammatory cytokines

The degradation of the epithelial barrier originates from dysregulated mucosal immune responses, which in turn exacerbate barrier dysfunction and trigger macrophage activation, driving the production of inflammatory cytokines during IBD pathogenesis[29]. Inflammatory cytokines are categorized into pro-inflammatory (such as IL-6, IL-1β, and TNF-α) and anti-inflammatory (such as IL-10) subtypes according to their distinct roles in immune and inflammatory processes. Studies have demonstrated that IL-6, IL-1β, and TNF-α are commonly associated with IBD and have been widely utilized as biomarkers to evaluate disease severity[30]. Results shown in Fig. 3B–E indicate that, compared with NC, pro-inflammatory cytokines (TNF-α, IL-6, and IL-1β) were significantly elevated ($P < 0.0001$), while the anti-inflammatory cytokine (IL-10) was markedly reduced ($P < 0.0001$) in MC, suggesting the systemic circulatory inflammation in mice. Upon beef tripe peptides treatments (NL, GL, and HS), the abnormal levels of pro-inflammatory cytokines (TNF-α, IL-6, and IL-1β) and the anti-inflammatory cytokine (IL-10) in the serum of UC mice were significantly reversed ($P < 0.05$), demonstrating that beef tripe peptides alleviated inflammatory status in UC mice. These were closely related to the infiltration of inflammatory cells. However, the anti-inflammatory activities of these three beef tripe peptides differ, with may be attributed to differences in

their amino acid compositions. Hydrophobic amino acids, such as leucine (Leu), proline (Pro), and alanine (Ala), are more prevalent in anti-inflammatory peptides[31]. A higher proportion of hydrophobic amino acids in the amino acid sequences of bioactive peptides correlates with enhanced anti-inflammatory effects, which explains why NL exhibits stronger anti-inflammatory activity. Food-derived bioactive peptides have been found to reduce the levels of pro-inflammatory cytokines (IL-1β, TNF-α, IL-8, and IL-6) in the serum of colitis mice to alleviate DSS-induced colitis[32]. In addition, prior studies have reported that an increase in the level of anti-inflammatory cytokine IL-10 can ameliorate DSS-induced colitis in mice[33].

TNF-α triggers the expression of multiple genes, exacerbating intestinal inflammation through three mechanisms: enhancing leukocyte recruitment via upregulation of adhesion molecules, stimulating pro-inflammatory cytokine secretion, and promoting nitric oxide (NO) production to increase vascular permeability[34]. IL-10 binds to its cognate receptor (IL-10R), subsequently suppressing TNF-α production and pro-inflammatory signaling via receptor's downstream pathways through multiple mechanisms[35]. Furthermore, IL-10 knockout mice exhibit mucosal/submucosal thickening and inflammatory cell infiltration, highlighting the critical role of IL-10 in maintaining intestinal immune homeostasis[36]. Taken together, we deduced that the beef tripe peptides exhibit anti-inflammatory properties and alleviate UC symptoms primarily through reducing the secretion of pro-inflammatory cytokines (TNF-α, IL-6, and IL-1β) in cells.

3.5 Effect of beef tripe peptides on the inflammatory cell infiltration in colitis

The recruitment of macrophages and neutrophils represents a key pathological hallmark of DSS-induced colitis, reflecting exacerbated inflammation and tissue damage[37]. To validate the aforementioned hypothesis and further analyze how beef tripe peptides influence colonic inflammatory cell infiltration, specific immunohistochemical staining for macrophages (F4/80) and neutrophils (Ly6G) was performed on the colonic tissue. The recruitment of leukocytes, particularly Ly6G neutrophils, is critical for initiating and sustaining inflammatory responses in colonic tissues[38, 39]. Ly6G neutrophils exhibited the strongest responsiveness to DSS-induced increases in cell populations, coinciding with a significant reduction in macrophage proportions within the bone marrow niche[40, 41]. The results are shown in Fig. 4, compared with NC, DSS-treated mice exhibited extensive infiltration of $F4/80^+$ macrophages (Fig. 4A&C) and $Ly6G^+$ neutrophiles (Fig. 4B&D) in colonic tissues, with extremely significant differences ($P < 0.0001$). Notably, intervention with beef tripe peptides induced a significant reduction in macrophage- and neutrophil-positive cell numbers ($P < 0.0001$). This phenomenon further validated the reliability of the MPO activity assay results presented in section 3.3 of this paper. The changes in MPO activity already demonstrated variations in the degree of cell infiltration. As expected, beef tripe peptides markedly counteracted DSS-induced macrophage and neutrophil infiltration, corroborating prior experimental evidence[42]. These results demonstrated that the treatments of beef tripe peptides exerted robust protective effects on intestinal barrier integrity.

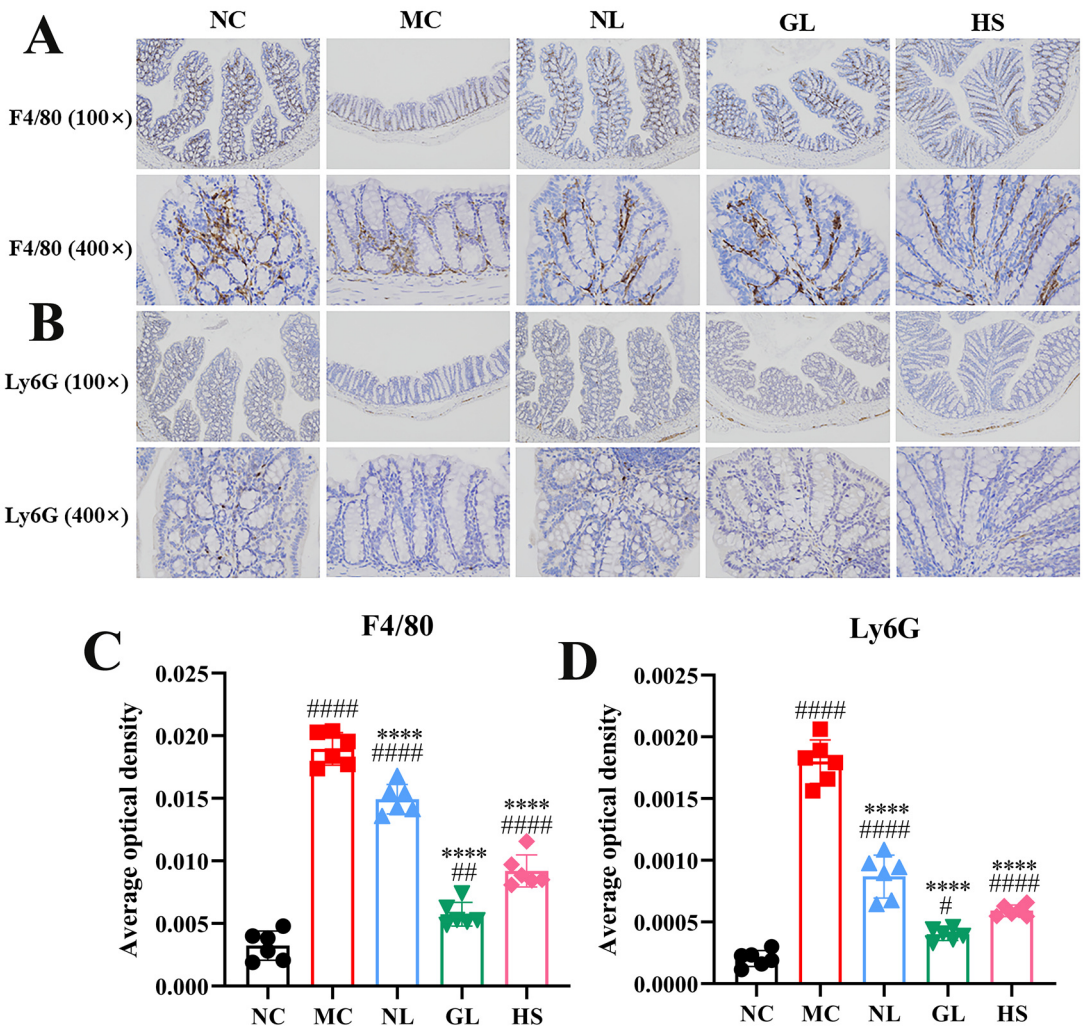

Fig. 4. Immunohistochemical analyses of F4/80 and Ly6G. A. Representative images of F4/80-stained tissue sections (magnification 100× and 400×). B. Representative images of Ly6G -stained tissue sections (magnification 100× and 400×). C. Average optical density values of F4/80 from each group. D. Average optical density values of Ly6G from each group. Note: $^{\#}P < 0.05$, $^{\#\#}P < 0.01$, $^{\#\#\#\#}P < 0.0001$ vs. NC; $^{****}P < 0.0001$ vs. MC.

3.6 Effect of beef tripe peptides on intestinal mucosal barrier function

The intestinal mucosal barrier comprises physical, chemical, microbiota, and immune barriers[43]. The physical barrier is formed by the intestinal epithelium, anchored by tight junction proteins, such as zonula occludens-1 (ZO-1), occludin, and claudin-1, and reinforced by a mucus layer derived from Paneth cell-secreted Mucin 2 (Muc-2). This mucus physically prevents pathogen and antigen invasion[44, 45]. Therefore, to investigate the protective effects of beef tripe peptides on the physical barrier of the intestinal mucosa in colitis-induced mice, we detected the mRNA expression levels of tight junction proteins in colonic tissues. As shown in Fig. 5A–C, compared with NC, DSS-induced mice exhibited a significant downregulation of mRNA expression of junction proteins (ZO-1, occludin, and claudin-1) in colonic tissues, with extremely significant differences ($P < 0.0001$). The diminished mRNA expression of these physical barrier components indicates compromised functional integrity of the colonic epithelial barrier[46]. Previous studies indicated that diminished expression of tight junction-associated proteins was correlated with neutrophil infiltration[47], which was consistent with the results presented in section 3.5 of this paper. After the treatments of beef tripe peptides, the mRNA expression levels of junction proteins increased significantly ($P <$

0.01) compared with MC. In addition, the mRNA expression of mucins in colonic tissues was evaluated (Fig. 5D). Notably, beef tripe peptides significantly upregulated Muc-2 mRNA expression, demonstrating extremely significant differences ($P < 0.0001$) compared with MC. Intestinal barrier dysfunction initiates a series of inflammatory cascades in colonic tissues[48]. In our study, mice with colitis exhibited overproduction of pro-inflammatory cytokines (TNF-α, IL-6, and IL-1β) and MPO, alongside downregulation of the anti-inflammatory cytokine IL-10. However, beef tripe peptides significantly reversed this pathological trend.

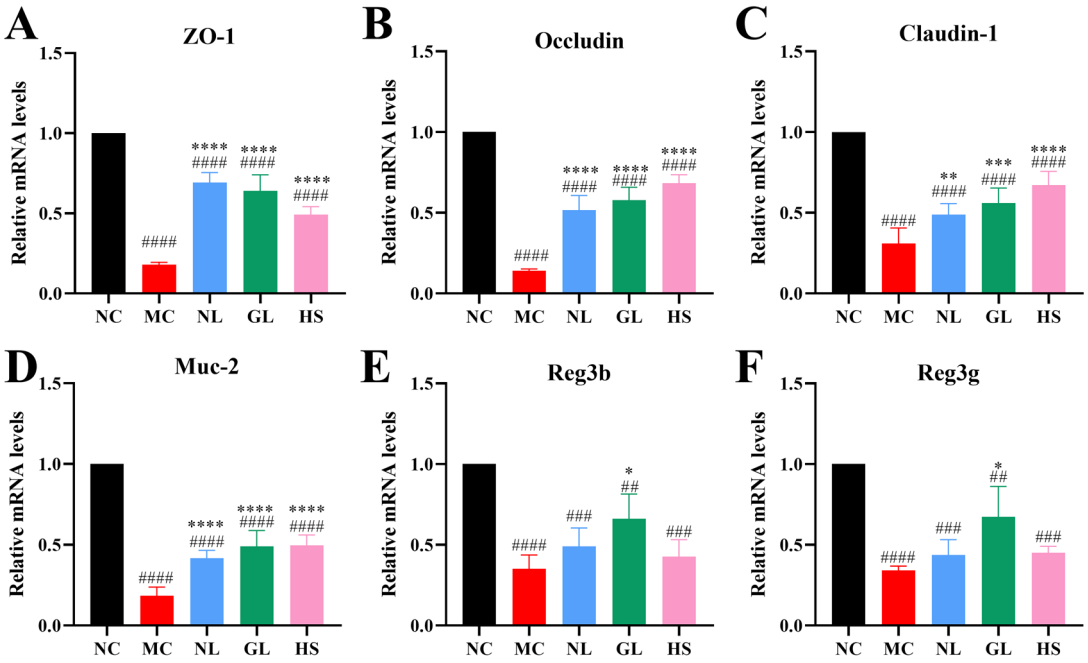

Fig. 5. Effects of beef tripe peptides on intestinal mucosal barrier function in mice with colitis: (A) ZO-1; (B) Occludin; (C) Claudin-1; (D) Muc2; (E) Reg3b; (F) Reg3g. Note: $^{\#\#}P < 0.01$, $^{\#\#\#}P < 0.001$, $^{\#\#\#\#}P < 0.0001$ vs. NC; $^{*}P < 0.05$, $^{**}P < 0.01$, $^{***}P < 0.001$, $^{****}P < 0.0001$ vs. MC.

Recombinant regenerating islet derived protein 3 (Reg3), a recombinant antimicrobial protein secreted by intestinal epithelial cells, functions as an essential constituent of the intestinal chemical barrier[49, 50]. To evaluate the protective effects of beef tripe peptides on the intestinal chemical barrier in colitis mice, we analyzed the mRNA expression levels of Reg3b and Reg3g in colonic tissues using qRT-PCR (Fig. 5E&F). The results showed that the mRNA expression levels of antimicrobial peptides Reg3b and Reg3g were significantly reduced in MC ($P < 0.0001$) compared with NC. However, beef tripe peptides significantly enhanced the expression levels of Reg3b and Reg3g in colonic tissues, but this increase was only statistically significant in GL ($P < 0.05$). Our results indicated that beef tripe peptides effectively counteracted the elevated intestinal permeability observed in UC model mice and reinstated the defensive capacity of the intestinal barrier. Collectively, these results strongly indicated that the protective mechanism of beef tripe peptides against UC was attributed to their ability to enhance the functional integrity of both the intestinal and mucus barriers.

3.7 Effect of beef tripe peptides on the related proteins of MAPK signaling pathway

Research findings consistently indicate that the MAPK signaling pathway is crucial in regulating intestinal inflammation and is closely associated with the expression of inflammatory factors[51, 52]. Therefore,

to further elucidate the potential mechanisms underlying the effects of beef tripe peptides on UC, western blotting was employed to investigate the impact of beef tripe peptides on the MAPK signaling pathway in colonic tissues of mice with UC. The MAPK subfamily comprises three key members: ERK, p38, and JNK, which are critical regulators in the modulation of inflammatory and immune responses[53]. Inflammatory factors such as TNF-α, IL-6, and IL-1β described in section 3.4 can all activate this signaling pathway[54]. As shown in Fig. 6, the results demonstrated that the phosphorylation levels of JNK, ERK, and p38 in MC were significantly upregulated ($P < 0.0001$), thereby confirming that DSS triggered activation of the MAPK signaling pathway. Following intervention with beef tripe peptides, the expression of these phosphorylated proteins was significantly reduced ($P < 0.01$, Fig. 6A–D), indicating that beef tripe peptides suppress inflammatory responses by inhibiting the MAPK signaling pathway. The anti-inflammatory effects of bioactive peptides are closely correlated with their amino acid composition. Notably, food-derived peptides rich in positively charged amino acids, such as lysine (Lys), arginine (Arg), and histidine (His), have been shown to possess potent anti-inflammatory capacities. These amino acids facilitate peptide interaction with the surface of target cell membranes, thereby enhancing their ability to modulate inflammatory signaling pathways[55, 56]. Peptides enriched with Leu and isoleucine (Ile) can effectively alleviate inflammatory responses by modulating kinase-mediated phosphorylation pathways[57].

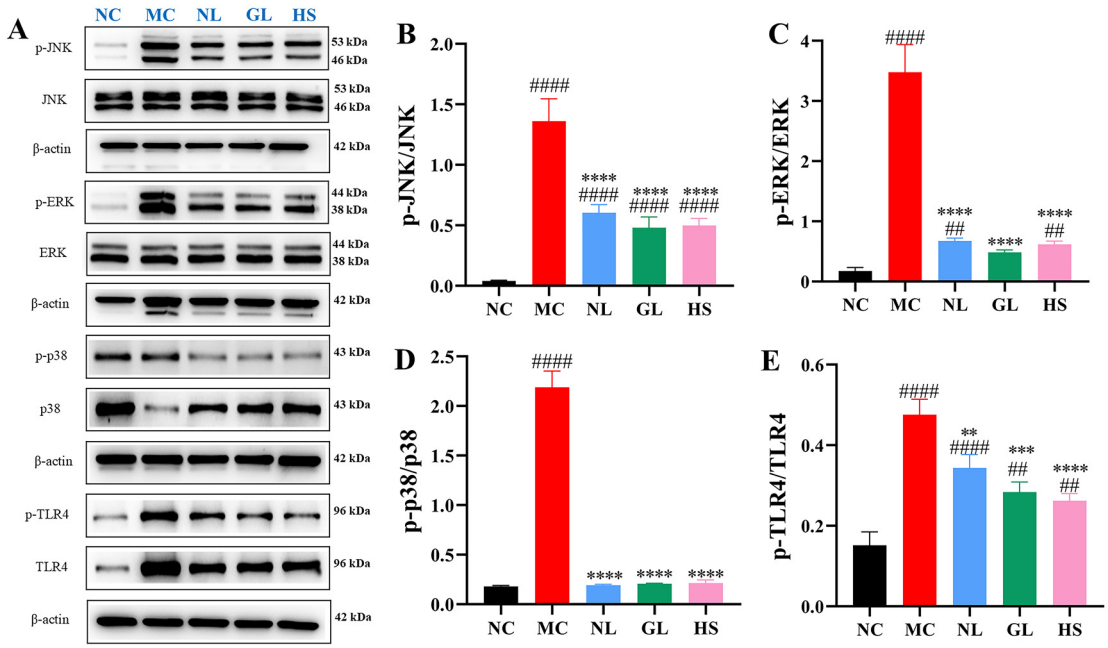

Fig. 6. Beef tripe peptides regulated MAPK signaling pathway activation in colonic tissue of DSS-induced colitis mice. A. Western blot analysis of the protein gel of MAPK signaling pathway. B–I. Histogram expressed as fold changes in protein expression normalized to β-actin expression. Note: $^{\#}P < 0.05$, $^{\#\#\#}P < 0.001$, $^{\#\#\#\#}P < 0.0001$ vs. NC; $^{*}P < 0.05$, $^{***}P < 0.001$, $^{****}P < 0.0001$ vs. MC.

TLR4 receptors are expressed on multiple cell types and play a critical role in inflammatory regulation[58]. Upon activation, TLR4 recruits MyD88, which subsequently activates the downstream MAPK signaling pathway to induce the release of inflammatory cytokines[59]. As shown in Fig. 6A&E, DSS significantly upregulated the phosphorylation level of TLR4 ($P < 0.0001$), while beef tripe peptides notably suppressed the phosphorylation of TLR4 ($P < 0.01$). These findings suggested that beef tripe peptides could

inhibit TLR4 activation, thereby suppressing downstream pro-inflammatory signaling cascades. In summary, these results demonstrated that beef tripe peptides exerted anti-inflammatory effects through the inhibition of the MAPK signaling pathway.

In our study, we induced colitis in mice using 3% DSS. DSS damages intestinal epithelial cells (IECs), disrupting intercellular tight junctions (mediated by ZO-1, occludin, and claudin-1) and depleting the mucin layer (Muc-2), which physically blocks microbiota invasion[45, 60]. These disruptions impaired the colonic barrier, triggering inflammatory responses. Beef tripe peptides restored mRNA expression of barrier proteins (ZO-1, claudin-1, occludin) and Muc-2 in colitis mice. Inflammatory markers, including elevated pro-inflammatory cytokines (TNF-α, IL-6, IL-1β), MPO activity (indicating neutrophil infiltration), and reduced anti-inflammatory IL-10, were reversed by beef tripe peptides. Macrophage and neutrophil infiltration—hallmarks of DSS colitis—was assessed via $F4/80^+$ (macrophages) and $Ly6G^+$ (neutrophils) staining, confirming peptide-mediated inhibition of inflammation[37]. Our findings show that beef tripe peptides protect colonic barrier integrity, counteracting DSS-induced inflammation. This is critical because barrier dysfunction initiates colonic inflammation, enabling microbial and inflammatory mediator invasion, which further amplifies cytokine-driven inflammation through a self-reinforcing cycle.

3.8 Effect of beef tripe peptides on the gut metabolites in DSS-induced mice

To clarify the regulatory effect of beef tripe peptides on gut metabolites in colitis mice model, non-target metabolomics technology was employed to identify metabolic changes in the intestinal contents of the mice. A total of 14705 metabolites were identified across all samples, including 7446 in the positive ion mode and 7259 in the negative ion mode. Cluster analysis was performed on the five sample groups, as shown in Fig. 7A. Samples within each group clustered closely together, demonstrating strong internal correlation, which validates their suitability for subsequent analyses. At the same time, the principal component analysis (PCA) score plot is shown in Fig. 7B. The distinct metabolic divergence observed between MC and NC underscored the disrupted metabolic profile in UC mice, which notably shifted toward NC following oral beef tripe peptides administration. Variable importance in projection (VIP) is a commonly used method for evaluating variable contributions in metabolic analysis[61]. A VIP score greater than 1 is generally considered statistically significant, so the criteria of $P < 0.05$ and VIP > 1 were applied to screen differentially abundant metabolites between pairwise comparison groups. The results are presented in Fig. 7C. A total of 725 substances were down-regulated, while 108 were up-regulated in MC compared with NC. Compared with MC, NL exhibited 884 down-regulated metabolites and 148 up-regulated metabolites, GL demonstrated 350 down-regulated metabolites and 341 up-regulated metabolites, and HS presented 451 up-regulated metabolites and 330 down-regulated metabolites. Volcano plots were performed for differentially abundant metabolites between pairwise comparison groups (Fig. 7D), enabling a visual assessment of their overall distribution. On the x-axis ($\log_2$ FC), the fold-change in metabolite expression between the two groups is plotted, while the y-axis displays the statistical significance of expression changes. Each point reflects an individual metabolite, with point size proportional to the VIP score, reflecting its contribution to group separation. The results

demonstrated that these three beef tripe peptides (NL, GL, and HS) exerted distinct metabolic regulatory effects in colitis mice, with differential modulation patterns on metabolite profiles.

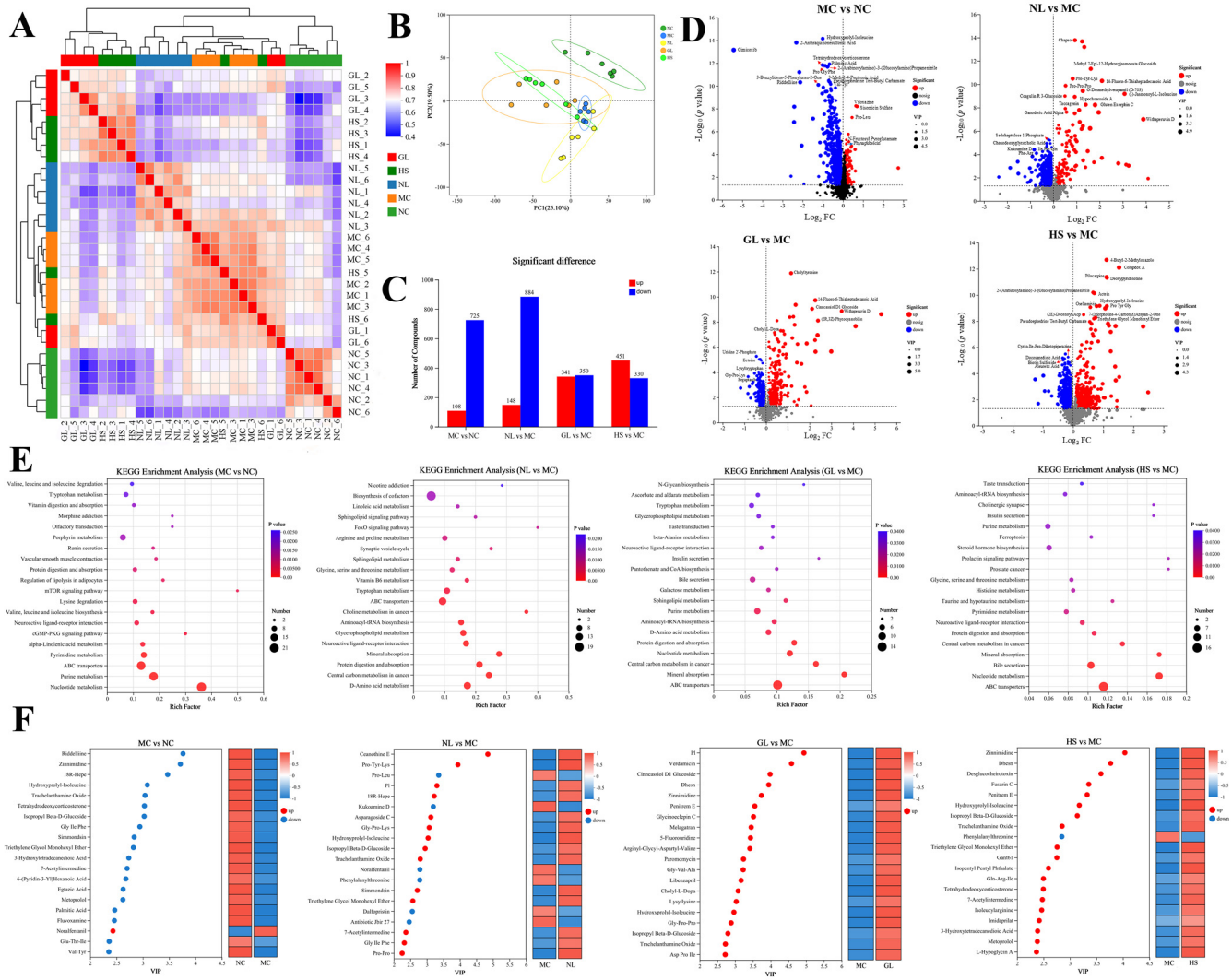

Fig. 7. Gut metabolomics revealed the regulation of metabolites by beef tripe peptides in UC mice. A. The heatmap of gut metabolites. B. PCA score plot. C. Differential metabolites quantity statistics plot. D. Volcano plots of differential metabolites. E. Top 20 KEGG pathways of differential metabolites. F. Top 20 VIP scores of differential metabolites.

To further explore the mechanisms underlying beef tripe peptides' improvement of intestinal barrier function in mice, KEGG pathway enrichment analysis was applied to profile the enriched metabolic pathways linked to significantly altered metabolite abundances. The top 20 KEGG pathways (ranked by significance) for each comparison group are presented in Fig. 7E. Compared with NC, colitis significantly impacted several metabolic pathways in mice, including nucleotide metabolism, purine metabolism, ABC transporters, pyrimidine metabolism, and alpha-linolenic acid metabolism. Nucleotide metabolism is influenced by the expression of ERK, where ERK activation stimulates the transcriptional activity of MYC. MYC is recognized as a major regulator of nucleotide metabolism, directly controlling the expression of genes involved in pyrimidine and purine synthesis[62]. This is consistent with the results in section 3.6 of this study, where hyperphosphorylation of ERK in colitis mice impaired their nucleotide metabolism. ATP-binding cassette (ABC) transporters constitute one of the largest families of membrane transporters and are ubiquitously distributed across diverse eukaryotic species[63]. Their critical role in immune defense has driven increasing

scientific interest, as highlighted by extensive research into their functional mechanisms[64-66]. Specifically, ABCF1 has been shown to participate in TLR4 signaling during innate immune responses in mouse macrophages, modulating the transition between MyD88-dependent and TIR-domain-containing adapter-inducing interferon-β (TRIF)-dependent signaling pathways to promote interferon β production[67]. However, colitis disrupted the immune defense system in mice, thereby impairing the functions of ABC transporters. Compared with MC, NL alleviated colonic inflammation in mice by modulating metabolite production through effects on protein digestion and absorption, neuroactive ligand-receptor interaction, ABC transporters, and tryptophan metabolism. At the same time, GL changed ABC transporters, nucleotide metabolism, protein digestion and absorption, purine metabolism, neuroactive ligand-receptor interaction, and tryptophan metabolism. HS changed ABC transporters, nucleotide metabolism, protein digestion and absorption, neuroactive ligand-receptor interaction, pyrimidine metabolism, and purine metabolism.

Fig. 7F shows the top 20 differentially abundant metabolites between pairwise comparison groups ($P < 0.05$), ranked by VIP scores. The results demonstrated that these three drug groups exhibited distinct metabolite expression patterns, with notable changes observed in the expression levels of some short peptides. Compared with NC, the short peptides Gly-Ile-Phe, Glu-Thr-Ile, and Val-Tyr were significantly downregulated in MC ($P < 0.05$). This might be due to DSS-induced inflammation in the colitis model mice, which activated inflammatory cytokines (such as TNF-α, IL-1β) and oxidative stress, potentially interfering with intestinal proteolysis or peptide synthesis pathways[68]. Compared with MC, the NL exhibited significantly upregulated levels of Pro-Tyr-Lys, Gly-Pro-Lys, Gly-Ile-Phe, Pro-Pro, and Hyp-Ile, while Pro-Leu was significantly downregulated. In contrast, the GL demonstrated marked upregulation of Gly-Val-Ala, Hyp-Ile, Gly-Pro-Pro, Asp-Pro-Ile, Arg-Gly-Asp-Val, and Lys-Lys. Meanwhile, the HS showed significant upregulation of Hyp-Ile, Gln-Arg-Ile, and Ile-Arg, whereas Phe-Thr exhibited a significant downregulation. The observed differences might be attributable to variations in the amino acid composition and the distinct sites of action of the functional residues among the three active peptides derived from beef tripe.

3.9 Correlation analysis between UC-related indicators and gut metabolites

Following treatment with beef tripe peptides, the expression levels of 55 metabolites in DSS-induced colitis mice were significantly reversed ($P < 0.05$) compared to the mice in MC. These 55 metabolites were regarded as the key metabolites of beef tripe peptides against UC, including phosphate esters, ethers, fatty acids, tricarboxylic acids, carbohydrates, amino acids, and peptides, etc. (Table 2). To clarify the relationship between the identified key metabolites and body weight, colon length, DAI, intestinal barrier indexes, and inflammatory indexes of UC mice, Spearman's correlation was performed, with the results visualized in a heatmap (Fig. 8). The results showed that tetrahydrodeoxycorticosterone (THDOC), 3-hydroxytetradecanedioic acid, 15-deacetylneosolaniol, and palmitic acid were significantly positively correlated with body weight of mice ($P < 0.05$), while lucidenic acid D2 and lintitript exhibited significant negative correlations ($P < 0.05$). THDOC is an effective positive allosteric modulator of the

gamma-amino-butyric-acid (GABA) type A receptor[69, 70]. In preclinical studies, THDOC showed a rapid increase under acute stress conditions[70], which might relate to the rapid weight loss in mice caused by inflammatory responses in this study, thereby triggering a protective mechanism within the mice's bodies. Changes in THDOC concentrations might be associated with alterations in the hypothalamic–pituitary–adrenal (HPA) system[71]. In healthy individuals, the levels of organic acids within the intestinal microenvironment are regulated to remain within a relatively stable range. Excessive harmful organic acids can cause damage to the intestinal tract[72]. In our study, we found that the level of 3-hydroxytetradecanedioic acid was significantly reduced in the MC, and beef tripe peptides could reverse this change. Palmitic acid originates from dietary sources or is synthesized endogenously from excess energy derived from carbohydrate and/or protein intake[73]. This fatty acid increases low-density lipoprotein cholesterol (LDL-C)[74], thereby promoting overweight/obesity. This mechanism explains its strong correlation with the body weight of mice. Lucidenic acid D2 is a secondary metabolite of *Ganoderma* genus. As reported, lucidenic acid has been shown to inhibit the activity of eukaryotic DNA polymerase[75]. Lintitript is a highly specific and potent antagonist of the cholecystokinin (CCK)-A receptor, which can accelerate the solid gastric emptying[76].

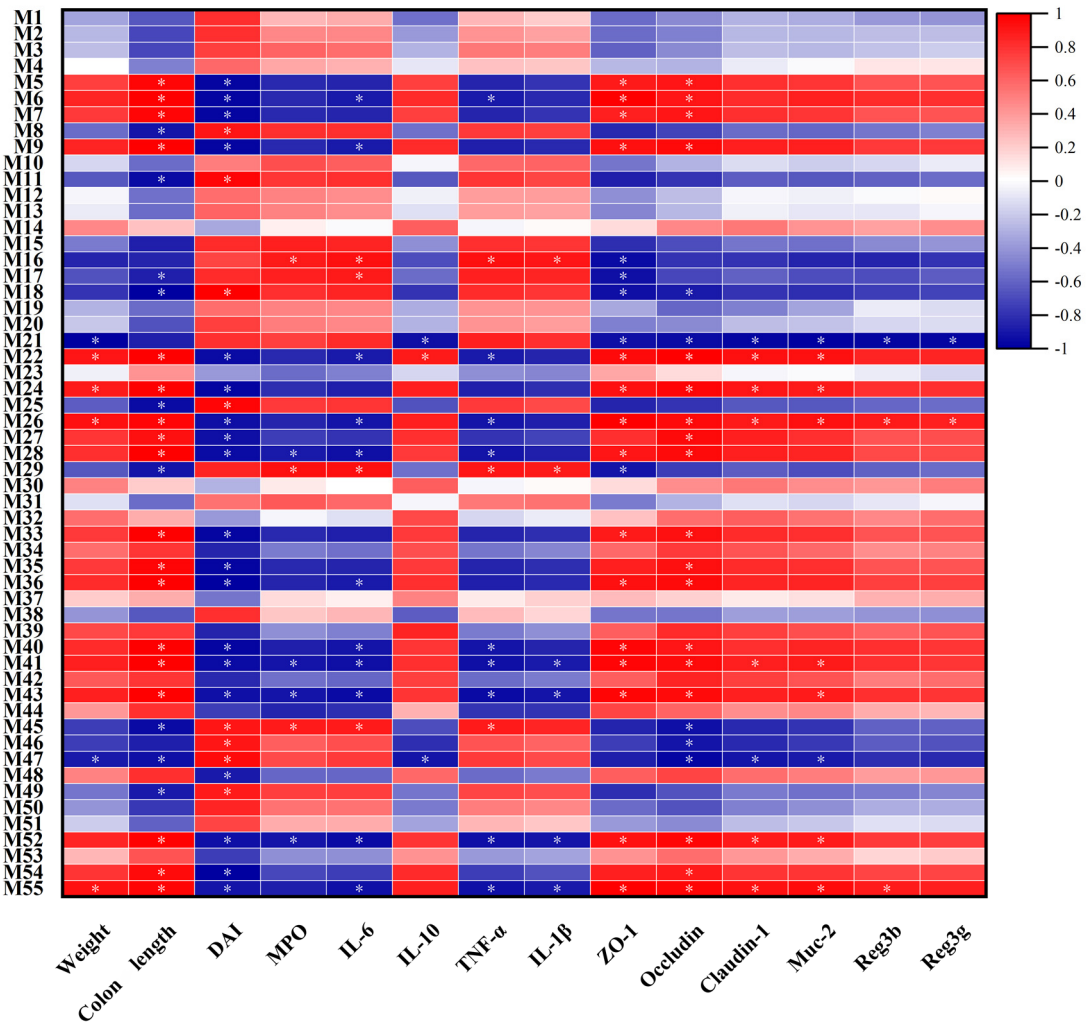

Fig. 8. Correlation analysis heatmap of UC-related indicators and differential metabolites. The y-axis shows the distinct metabolites in Table 2. Note: $^{*}P < 0.05$.

Table 2 The identification of differential metabolites based on gut metabolomics.

No.	RT. (min)	Ion mode	Metabolites	Formula	MC/NC			NL/MC			GL/MC			HS/MC		
					VIP	FC	Trend	VIP	FC	Trend	VIP	FC	Trend	VIP	FC	Trend
M1	0.64215	+	Ectoine	$C_6H_{10}N_2O_2$	1.10	1.09	##↑	1.52	0.90	**↓	2.08	0.83	****↓	1.21	0.92	*↓
M2	0.649983	+	N-Acetylputrescine	$C_6H_{14}N_2O$	1.13	1.10	##↑	1.62	0.84	**↓	1.75	0.83	***↓	1.42	0.88	**↓
M3	0.6733	+	N-Acetylhistamine	$C_7H_{11}N_3O$	1.18	1.19	#↑	2.20	0.71	***↓	1.71	0.77	*↓	1.50	0.83	*↓
M4	0.681117	+	Phenylalanylthreonine	$C_{13}H_{18}N_2O_4$	1.37	1.19	##↑	2.78	0.52	**↓	2.56	0.56	**↓	2.85	0.52	**↓
M5	0.9318	+	Isopropyl Beta-D-Glucoside	$C_9H_{18}O_6$	3.03	0.46	###↓	2.95	1.92	**↑	2.79	1.91	**↑	3.14	1.97	***↑
M6	0.994417	+	N-(3-Hydroxypropyl)Valine	$C_8H_{17}NO_3$	1.95	0.81	####↓	1.67	1.16	**↑	1.58	1.16	**↑	1.49	1.12	**↑
M7	1.082233	+	Hydroxyprolyl-Isoleucine	$C_{11}H_{20}N_2O_4$	3.09	0.50	####↓	3.04	1.78	****↑	2.96	1.79	****↑	3.17	1.84	****↑
M8	1.842017	+	Val Val	$C_{10}H_{20}N_2O_3$	1.22	1.10	##↑	1.51	0.89	**↓	1.15	0.91	*↓	1.13	0.93	**↓
M9	2.571683	+	7-Acetylintermedine	$C_{17}H_{27}NO_6$	2.70	0.64	####↓	2.36	1.38	***↑	2.35	1.40	***↑	2.48	1.39	****↑
M10	2.7649	+	Pro-Leu	$C_{11}H_{20}N_2O_3$	2.06	1.37	####↑	3.36	0.35	**↓	1.88	0.77	**↓	1.80	0.81	**↓
M11	2.832633	+	Estriol	$C_{18}H_{24}O_3$	1.55	1.14	###↑	1.79	0.87	***↓	1.59	0.88	**↓	1.44	0.90	**↓
M12	2.845417	+	Antibiotic Jbir 27	$C_{15}H_{22}O_3$	1.10	1.10	##↑	2.46	0.71	***↓	1.82	0.81	**↓	1.60	0.85	**↓
M13	2.90835	+	Triacanthine	$C_{10}H_{13}N_5$	1.06	1.09	###↑	2.08	0.76	**↓	1.71	0.83	**↓	1.48	0.89	****↓
M14	2.90835	+	Asn-Glu-Ile	$C_{15}H_{26}N_4O_7$	1.00	0.90	#↓	1.33	0.86	*↓	1.26	1.12	*↑	1.48	1.15	*↑
M15	5.125017	+	4-Chloro-2-Nitrobenzylalcohol	$C_{29}H_{37}N_3O_6$	1.88	1.34	##↑	2.40	0.67	**↓	1.69	0.80	*↓	1.66	0.80	*↓
M16	5.711317	+	Sisomicin Sulfate	$C_{19}H_{37}N_5O_7$	2.74	1.62	####↑	2.13	0.76	*↓	1.52	0.88	***↓	1.13	0.93	*↓
M17	5.721233	+	Desacetoxyvindoline	$C_{23}H_{30}N_2O_4$	2.05	1.34	####↑	2.05	0.75	*↓	1.63	0.84	**↓	1.18	0.91	*↓
M18	6.768083	+	7-O-Methylbavachin	$C_{21}H_{22}O_4$	1.18	1.11	##↑	1.22	0.92	**↓	1.07	0.92	*↓	1.03	0.94	*↓
M19	6.91675	+	Bilirubin	$C_{33}H_{36}N_4O_6$	1.52	1.14	##↑	1.76	0.88	***↓	1.60	0.88	**↓	2.52	0.73	**↓
M20	7.777083	+	Kukoamine C	$C_{28}H_{42}N_4O_6$	1.12	1.11	#↑	2.04	0.82	***↓	1.88	0.83	***↓	1.93	0.85	***↓
M21	6.650667	+	Lucidenic Acid D2	$C_{29}H_{38}O_8$	2.22	1.53	##↑	1.38	0.89	**↓	1.62	0.85	**↓	1.44	0.89	**↓
M22	4.896783	+	Tetrahydrodeoxycorticosterone	$C_{21}H_{34}O_3$	3.03	0.49	####↓	2.23	1.57	**↑	2.40	1.63	***↑	2.49	1.62	**↑
M23	4.66185	+	Milbemycin Alpha5	$C_{38}H_{56}O_{10}$	1.26	0.70	#↓	3.81	2.79	****↑	1.89	1.60	**↑	1.89	1.64	*↑
M24	4.56285	+	3-Hydroxytetradecanedioic Acid	$C_{14}H_{26}O_5$	2.73	0.54	####↓	2.10	1.49	**↑	2.33	1.58	***↑	2.39	1.57	***↑
M25	4.41195	+	Physapubescin	$C_{30}H_{42}O_8$	1.33	1.12	####↑	1.44	0.89	***↓	1.38	0.89	***↓	1.35	0.91	***↓
M26	4.21745	+	Palmitic Acid	$C_{16}H_{32}O_2$	2.47	0.63	####↓	1.75	1.34	*↑	1.81	1.34	**↑	1.72	1.27	**↑
M27	4.125067	+	Trp-Pro	$C_{16}H_{19}N_3O_3$	1.70	0.78	##↓	1.28	1.17	**↑	1.48	1.21	*↑	1.82	1.25	**↑
M28	4.099617	+	Triethylene Glycol Monohexyl Ether	$C_{12}H_{26}O_4$	2.82	0.55	####↓	2.57	1.59	****↑	2.25	1.52	***↑	2.76	1.61	****↑
M29	2.8582	+	Noralfentanil	$C_{16}H_{24}N_2O_2$	2.43	1.51	####↑	2.79	0.64	***↓	2.04	0.79	***↓	2.08	0.81	***↓
M30	2.7805	+	Asn-Asp-Leu	$C_{14}H_{24}N_4O_7$	1.74	0.75	#↓	2.34	0.51	*↓	1.65	1.30	*↑	1.98	1.35	*↑
M31	2.7649	+	Spectinomycin	$C_{14}H_{24}N_2O_7$	1.28	1.11	##↑	2.45	0.73	**↓	1.48	0.88	**↓	1.37	0.90	*↓
M32	2.72025	+	Starch Acetate	$C_{12}H_{18}O_9$	1.38	0.85	###↓	1.23	0.85	*↓	1.16	1.14	*↑	1.49	1.18	*↑
M33	2.457	+	3,7,8,15-Scirpenetetrol	$C_{15}H_{22}O_6$	2.83	0.61	####↓	2.70	1.48	****↑	2.61	1.48	****↑	2.90	1.52	****↑
M34	2.409083	+	L-Phenylalanine	$C_9H_{11}NO_2$	1.76	0.65	#↓	1.69	1.36	*↑	2.23	1.62	*↑	2.34	1.70	*↑
M35	2.05165	+	2-(Arabinosylamino)-3-(Glucosyl	$C_{14}H_{25}N_3O_9$	2.82	0.59	####↓	2.68	1.52	****↑	2.62	1.53	****↑	2.91	1.58	****↑

			amino)Propanenitrile												
M36	2.034717	+	Trachelanthamine Oxide	$C_{15}H_{27}NO_5$	3.04	0.55	####↓	2.80	1.58	***↑	2.72	1.59	***↑	2.85	1.58	****↑
M37	1.842017	+	Gly-Pro-Pro	$C_{12}H_{19}N_3O_4$	1.17	0.90	###↓	1.11	1.10	*↑	2.89	1.49	****↑	1.14	1.09	**↑
M38	1.650333	+	Tropine	$C_8H_{15}NO$	1.10	1.13	##↑	1.24	0.90	**↓	1.72	0.78	*↓	1.27	0.87	*↓
M39	0.9318	+	Isoleucylarginine	$C_{12}H_{25}N_5O_3$	2.24	0.66	####↓	1.20	1.18	*↑	2.62	1.54	****↑	2.46	1.51	**↑
M40	3.308133	–	Simmondsin	$C_{16}H_{25}NO_9$	2.84	0.51	####↓	2.71	1.70	****↑	2.47	1.65	***↑	2.22	1.51	**↑
M41	3.563733	–	6-(Pyridin-3-Yl)Hexanoic Acid	$C_{11}H_{15}NO_2$	2.68	0.51	###↓	2.20	1.65	*↑	1.93	1.57	*↑	2.14	1.56	*↑
M42	3.97295	–	Gamma-Glu-Leu	$C_{11}H_{20}N_2O_5$	1.73	0.82	###↓	1.20	1.11	*↑	1.66	1.21	**↑	2.09	1.26	**↑
M43	4.3747	–	Dioscoretine	$C_{13}H_{23}NO_3$	2.30	0.67	####↓	2.04	1.33	***↑	1.66	1.27	**↑	1.88	1.27	****↑
M44	4.5893	–	Val-Pro-Pro	$C_{15}H_{25}N_3O_4$	1.76	0.72	###↓	2.65	1.58	****↑	1.61	1.30	**↑	1.91	1.36	**↑
M45	4.643917	–	Morph	$C_{10}H_{16}N_2O_4$	1.83	1.29	####↑	1.73	0.83	**↓	1.43	0.86	**↓	1.86	0.80	**↓
M46	4.70435	–	Lysyltryptophan	$C_{17}H_{24}N_4O_3$	1.56	1.20	####↑	1.31	0.91	***↓	1.63	0.86	***↓	1.77	0.84	***↓
M47	4.70435	–	Lintitript	$C_{20}H_{14}ClN_3O_3S$	1.64	1.24	###↑	1.26	0.91	**↓	1.59	0.85	***↓	1.57	0.86	***↓
M48	5.89545	–	N-Desmethyl Topotecan	$C_{22}H_{21}N_3O_5$	1.38	0.83	###↓	1.43	1.20	**↑	1.57	1.25	**↑	1.66	1.27	**↑
M49	6.157767	–	Chenodeoxyglycocholic Acid	$C_{26}H_{43}NO_5$	1.60	1.18	###↑	2.02	0.81	****↓	1.52	0.84	*↓	1.37	0.89	*↓
M50	6.722683	–	Arctiin	$C_{27}H_{34}O_{11}$	1.49	1.19	#↑	1.82	0.82	**↓	1.97	0.79	**↓	2.11	0.77	**↓
M51	3.893767	–	Sedoheptulose 1-Phosphate	$C_7H_{15}O_{10}P$	1.04	1.10	###↑	1.67	0.85	****↓	1.79	0.80	***↓	1.88	0.82	****↓
M52	3.529267	–	Heptenophos	$C_9H_{12}ClO_4P$	1.49	0.84	####↓	1.22	1.13	**↑	1.13	1.11	**↑	1.35	1.13	***↑
M53	3.490933	–	Glycylprolylhydroxyproline	$C_{12}H_{19}N_3O_5$	1.06	0.85	#↓	1.44	1.21	*↑	1.53	1.28	*↑	1.71	1.32	*↑
M54	3.238583	–	Pro-Glu	$C_{10}H_{16}N_2O_5$	1.54	0.81	###↓	1.37	1.16	**↑	1.58	1.22	***↑	1.31	1.18	*↑
M55	0.675517	–	15-Deacetylneosolaniol	$C_{17}H_{24}O_7$	2.28	0.67	####↓	1.73	1.27	**↑	1.57	1.26	**↑	1.68	1.25	**↑

It was found that 27 key metabolites were significantly correlated with colon length of UC mice ($P < 0.05$), including isopropyl beta-D-glucoside, N-(3-hydroxypropyl)valine, hydroxyprolyl-isoleucine, Val-Val, 7-acetylintermedine, estriol, desacetoxyvindoline, 7-O-methylbavachin, tetrahydrodeoxycorticosterone, 3-hydroxytetradecanedioic acid, physapubescin, palmitic acid, Trp-Pro, triethylene glycol monohexyl ether, noralfentanil, 3,7,8,15-scirpenetetrol, 2-(arabinosylamino)-3-(glucosylamino)propanenitrile, trachelanthamine oxide, simmondsin, 6-(pyridin-3-Yl)hexanoic acid, dioscoretine, morph, lintitript, chenodeoxyglycocholic acid, heptenophos, Pro-Glu, and 15-deacetylneosolaniol. Estriol, a natural hormone, has been found in studies to alleviate the central nervous system (CNS) inflammation when used as treatment[77]. Physapubescin, a withanolide, has been identified as a highly efficient and specific inhibitor of the kidney-type glutaminase (KGA) enzyme. It demonstrated potent anticancer activity *in vitro* and suppressed tumor cell growth *in vivo*[78]. Simmondsin is a cyanomethylene glycoside that can reduce body weight and food intake in mice while exhibiting toxicity and adversely affecting the hematopoietic system[79]. Meanwhile, a total of 27 metabolites exhibited statistically significant correlations with DAI of UC mice ($P < 0.05$), including phenylalanylthreonine, isopropyl beta-D-glucoside, N-(3-hydroxypropyl)valine, hydroxyprolyl-isoleucine, Val-Val, 7-acetylintermedine, estriol, 7-O-methylbavachin, tetrahydrodeoxycorticosterone, 3-hydroxytetradecanedioic acid, physapubescin, palmitic acid, Trp-Pro, triethylene glycol monohexyl ether, 3,7,8,15-scirpenetetrol, 2-(arabinosylamino)-3-(glucosylamino)propanenitrile, trachelanthamine oxide, simmondsin, 6-(pyridin-3-Yl)hexanoic acid, dioscoretine, morph, lysyltryptophan, lintitript, N-desmethyl topotecan, chenodeoxyglycocholic acid, heptenophos, Pro-Glu, and 15-deacetylneosolaniol. Clinical studies have demonstrated that estriol treatment possesses anti-inflammatory and neuroprotective properties, primarily mediated through the binding of estrogen receptors expressed in the immune system and central nervous system[80], thereby regulating the DAI in mice.

Sisomicin sulfate, noralfentanil, and morph exhibited positive correlations with MPO activity of UC mice ($P < 0.05$). Meanwhile, triethylene glycol monohexyl ether, 6-(pyridin-3-Yl)hexanoic acid, dioscoretine, and heptenophos showed negative correlations with MPO activity ($P < 0.05$). Dioscoretine, derived from *Dioscorea deltoidei*, has been reported to possess preventive effects against rheumatic diseases and therapeutic activities against inflammation[81], thereby reducing the infiltration of inflammatory cells and affecting MPO activity. There were 17 metabolites that were significantly associated with the inflammatory cytokines (TNF-α, IL-6, IL-1β, and IL-10) in UC mice ($P < 0.05$), including N-(3-hydroxypropyl)valine, 7-acetylintermedine, sisomicin sulfate, desacetoxyvindoline, lucidenic acid D2, tetrahydrodeoxycorticosterone, palmitic acid, triethylene glycol monohexyl ether, noralfentanil, trachelanthamine oxide, simmondsin, 6-(pyridin-3-Yl)hexanoic acid, dioscoretine, morph, lintitript, heptenophos, and 15-deacetylneosolaniol. Palmitic acid-induced palmitoylation regulates protein function and impacts various pathophysiological process. Palmitoylated proteins are key modulators of inflammation and immune responses[82]. A total of 26 metabolites were found to be significantly correlated with proteins

critical for intestinal mucosal barrier function (ZO-1, occludin, claudin-1, Muc-2, and Reg3) of UC mice ($P < 0.05$), including isopropyl beta-D-glucoside, N-(3-hydroxypropyl)valine, hydroxyprolyl-isoleucine, Val-Val, 7-acetylintermedine, sisomicin sulfate, desacetoxyvindoline, 7-O-methylbavachin, lucidenic acid D2, tetrahydrodeoxycorticosterone, 3-hydroxytetradecanedioic acid, palmitic acid, Trp-Pro, triethylene glycol monohexyl ether, noralfentanil, 3,7,8,15-scirpenetetrol, 2-(arabinosylamino)-3-(glucosylamino)propanenitrile, trachelanthamine oxide, simmondsin, 6-(pyridin-3-Yl)hexanoic acid, dioscoretine, morph, lysyltryptophan, lintitript, heptenophos, Pro-Glu, and 15-deacetylneosolaniol. Sisomicin is an aminoglycoside antibiotic containing multiple amino and glycosyl groups, which binds to bacterial ribosomes to inhibit protein synthesis and thereby exerts antimicrobial activity[83]. The sulfate form enhances its water solubility and stability, making it more suitable for clinical applications.

In total, among these 55 key metabolites, 6 were significantly correlated with body weight, 27 with colon length, 27 with DAI, 7 with MPO activity, 17 with inflammatory cytokines, and 26 with proteins involved in intestinal mucosal barrier function in the UC mouse model. These findings collectively highlighted that the key mechanism underlying the therapeutic effect of beef tripe peptides for UC was to ameliorate metabolic dysfunction.

4. Conclusions

This study demonstrated that bioactive peptides from beef tripe (NLPLPPPPPPR, GLGPPSPPAPP, and HSLPPGPY) alleviated DSS-induced colitis in mice, improving DAI scores, reducing weight loss and colon shortening, and suppressing splenomegaly. Histologically, peptides restored colonic mucosal architecture, reduced inflammatory cell infiltration, and decreased histological damage. Specifically, they inhibited macrophage/neutrophil infiltration, MPO activity, and preserved colonic mucosal barriers. Mechanistically, peptides suppressed MAPK pathway activation (JNK/ERK/p38 phosphorylation) to block inflammation. Metabolomics revealed that the peptides reversed DSS-induced metabolic disturbances in mice. Collectively, these findings highlight the therapeutic potential of beef tripe peptides in managing UC, supporting their exploration as clinical or dietary interventions for IBD. Additionally, current studies on bioactive peptides in beef tripe only use cell or animal experiments, lacking human trials. Though animal tests (e.g. mice) can simulate human conditions, differences in their inflammation and metabolism may mean results can’t be directly applied to humans. Peptides effective in animal models may need retesting in humans for safety and dosage. Thus, more human studies are needed to understand how these peptides repair the intestinal barrier in people.

Declaration of Competing Interest

The authors declare no conflict of interest.

Data availability

Data will be made available on request.

Acknowledgements

This work was supported by Chongqing Technology Innovation and Application Development Special Key Project (Grant No. CSTB2022TIAD-KPX0080), Collaborative Innovation and Key Technology of Rabbit Industry in Sichuan and Chongqing (Grant No. 2022YFQ0033), and Agriculture Research System of China of MOF and MARA (Grant No. CARS-43-E-2).

References

[1] H. Lee, J.H. Lee, S.J. Koh, et al., Bidirectional relationship between atopic dermatitis and inflammatory bowel disease: A systematic review and meta-analysis. Journal of the American Academy of Dermatology 83(5) (2020) 1385–1394. https://doi.org/10.1016/j.jaad.2020.05.130.

[2] R. Ungaro, S. Mehandru, P.B. Allen, et al., Ulcerative colitis, The Lancet 389(10080) (2017) 1756–1770. https://doi.org/10.1016/s0140-6736(16)32126-2.

[3] L. Li, J. Li, S. Zhou, et al., Research progress of beef tripe processing industry, Guangdong Agricultural Sciences 22 (2011) 103–106. https://doi.org/10.16768/j.issn.1004-874x.2011.22.011.

[4] X. Sun, Z. He, L. Yang, et al., Quantitative proteomic analysis to identify potential biomarkers linked to quality traits of beef tripe from different sources, Food Chemistry (2024) 449 139224. https://doi.org/10.1016/j.foodchem.2024.139224.

[5] G.C. Zarkadas, C.D. Karatzas, C.G. Zarkadas, Assessing the myofibrillar and connective tissue protein contents and protein quality of beef tripe, Journal of Agricultural and Food Chemistry 44 (1996) 2563−2572.

[6] X. Sun, Z. He, L. Yang, et al., Effect of cooking treatment on protein digestibility, peptide profile and potential bioactive peptides of beef tripe during in vitro gastrointestinal digestion, Food Chemistry 470 (2025) 142720. https://doi.org/10.1016/j.foodchem.2024.142720.

[7] T. Zhang, C. Ma, Z. Zhang, et al., NF-κB signaling in inflammation and cancer, MedComm 2(4) (2021) 618–653. https://doi.org/10.1002/mco2.104.

[8] J. Wei, J. Feng, Signaling pathways associated with inflammatory bowel disease, Recent Patents on Inflammation & Allergy Drug Discovery 4 (2010) 105–117. https://doi.org/10.2174/187221310791163071.

[9] J.S.C. Arthur, S.C. Ley, Mitogen-activated protein kinases in innate immunity, Nature Reviews Immunology 13(9) (2013) 679–692. https://doi.org/10.1038/nri3495.

[10] Z.X. Zha, Y. Lin, K.X. Wang, et al., Hederacoside C ameliorates colitis via restoring impaired intestinal barrier through moderating S100A9/MAPK and neutrophil recruitment inactivation, Acta Pharmacologica Sinica 44 (2023) 105–119. https://doi.org/10.1038/s41401-022-00933-3.

[11] L. Qu, X. Lin, C. Liu, et al., Atractylodin attenuates dextran sulfate sodium-induced colitis by alleviating gut microbiota dysbiosis and inhibiting inflammatory response through the MAPK pathway, Frontiers in Pharmacology 12 (2021) 665376. https://doi.org/10.3389/fphar.2021.665376.

[12] Hwang, J. W., Lee, S. J., Kim, Y. S., et al., Purification and characterization of a novel peptide with inhibitory effects on colitis induced mice by dextran sulfate sodium from enzymatic hydrolysates of *Crassostrea gigas*, Fish & Shellfish Immunology 33 (2012) 993–999. https://doi.org/10.1016/j.fsi.2012.08.017.

[13] J. Feng, H. Wang, X. Luo, et al., Identification and molecular mechanism of the anti-inflammatory effect of sea cucumber peptides: Network pharmacology, molecular docking and animal experiments, International Journal of Biological Macromolecules 279 (2024) 134958. https://doi.org/10.1016/j.ijbiomac.2024.134958.

[14] T. Qu, Y. Wu, Z. Zhang, et al., From by-product to biopeptide: Insight into the anti-inflammatory mechanism of peptides from rice dreg via peptidomics, multi-in silico, and in vitro approaches, Journal of Future Foods (2025). https://doi.org/10.1016/j.jfutfo.2025.07.008.

[15] L. Yuan, Q. Chu, B. Yang, et al., Purification and identification of anti-inflammatory peptides from sturgeon (*Acipenser schrenckii*) cartilage, Food Science and Human Wellness 12 (2023) 2175–2183. https://doi.org/10.1016/j.fshw.2023.03.030.

[16] Y. Zhou, D. Wang, H. Duan, et al., Silkworm pupa protein peptide improved DSS-induced colitis in C57BL/6 mice through the MAPK/NF-κB signaling pathway, Journal of Functional Foods 110 (2023) 105852. https://doi.org/10.1016/j.jff.2023.105852.

[17] J. Hu, Y. Mei, H. Zhang, et al., Ameliorative effect of an acidic polysaccharide from Phellinus linteus on ulcerative colitis in a DSS-induced mouse model, International Journal of Biological Macromolecules 265 (2024) 130959. https://doi.org/10.1016/j.ijbiomac.2024.130959.

[18] Y. Liu, S. Deng, L. Sun, et al., Compound sophorae decoction mitigates DSS-induced ulcerative colitis by activating autophagy through PI3K-AKT pathway: A integrative research combining network pharmacology and in vivo animal model validation, Journal of Ethnopharmacology 337 (2025) 118885. https://doi.org/10.1016/j.jep.2024.118885.

[19] R. Han, H. He, Y. Lu, et al., Oral targeted drug delivery to post-gastrointestinal sites, Journal of Controlled Release 370 (2024) 256–276. https://doi.org/10.1016/j.jconrel.2024.04.047.

[20] A. Mehmood, S. Javaid, S.U. Rehman, et al., Exploring drug administration routes using chitosan-based polymeric nanoparticles: A comprehensive review, Journal of Drug Delivery Science and Technology 113 (2025) 107347. https://doi.org/10.1016/j.jddst.2025.107347.

[21] C. Brummer, K. Singer, K. Renner, et al., The spleen-liver axis supports obesity-induced systemic and fatty liver inflammation via MDSC and NKT cell enrichment, Molecular and Cellular Endocrinology 601 (2025) 112518. https://doi.org/10.1016/j.mce.2025.112518.

[22] Z. Chen, Y. Zhang, X. Zhang, et al., Anti-inflammatory effect of a novel millet gliadin peptide on mice with colitis, Journal of Functional Foods 111 (2023) 105912. https://doi.org/10.1016/j.jff.2023.105912.

[23] X. Fan, H. Zhou, W. Quan, et al., The highly stabilized biologically derived peptide VIESPPEI alleviates DSS-induced colitis in mice by preventing colonic atrophy and modulating gut microbiota, Food Bioscience 62 (2024) 105090. https://doi.org/10.1016/j.fbio.2024.105090.

[24] M. Van der Sluis, B.A.E. De Koning, A.C.J.M. De Bruijn, et al., Muc2-Deficient Mice Spontaneously Develop Colitis, Indicating That MUC2 Is Critical for Colonic Protection, Gastroenterology 131 (2006) 117–129. https://doi.org/10.1053/j.gastro.2006.04.020.

[25] T. Pelaseyed, J.H. Bergström, J.K. Gustafsson, et al., The mucus and mucins of the goblet cells and enterocytes provide the first defense line of the gastrointestinal tract and interact with the immune system, Immunological Reviews 260(1) (2014) 8–20. https://doi.org/10.1111/imr.12182.

[26] P. Guilpain, A. Servettaz, F. Batteux, et al., Natural and disease associated anti-myeloperoxidase (MPO) autoantibodies, Autoimmunity Reviews 7 (2008) 421–425. https://doi.org/10.1016/j.autrev.2008.03.009.

[27] S.M. Bastaki, E. Adeghate, N. Amir, et al., Menthol inhibits oxidative stress and inflammation in acetic acid-induced colitis in rat colonic mucosa, American Journal of Translational Research 10(12) (2018) 4210–4222.

[28] M. Rafeeq, H.A.S. Murad, H.M. Abdallah, et al., Protective effect of 6-paradol in acetic acid-induced ulcerative colitis in rats, BMC Complementary Medicine and Therapies 21 (2021) 28. https://doi.org/10.1186/s12906-021-03203-7.

[29] V. Svolos, R. Hansen, B. Nichols, et al., Treatment of Active Crohn's Disease With an Ordinary Food-based Diet That Replicates Exclusive Enteral Nutrition, Gastroenterology 156(5) (2019) 1354–1367. https://doi.org/10.1053/j.gastro.2018.12.002.

[30] M. Sarra, F. Pallone, T.T. MacDonald, et al., IL-23/IL-17 axis in IBD, Inflammatory Bowel Diseases 16(10) (2010) 1808–1813. https://doi.org/10.1002/ibd.21248.

[31] S. Guha, K. Majumder, Structural-features of food-derived bioactive peptides with anti-inflammatory activity: A brief review, Journal of Food Biochemistry 43 (2019) e12531. https://doi.org/10.1111/jfbc.12531.

[32] H. Ge, Z. Cai, J. Chai, et al., Egg white peptides ameliorate dextran sulfate sodium-induced acute colitis symptoms by inhibiting the production of pro-inflammatory cytokines and modulation of gut microbiota composition, Food Chemistry 360 (2021) 129981. https://doi.org/10.1016/j.foodchem.2021.129981.

[33] U. Jain, T.M. Woodruff, A.W. Stadnyk, The C5a receptor antagonist PMX205 ameliorates experimentally induced colitis associated with increased IL-4 and IL-10, British Journal of Pharmacology 168(2) (2012) 488–501. https://doi.org/10.1111/j.1476-5381.2012.02183.x.

[34] G. Bouguen, J.B. Chevaux, L. Peyrin-Biroulet, Recent advances in cytokines: Therapeutic implications for inflammatory bowel diseases, World Journal of Gastroenterology 17(5) (2011) 547–556. https://doi.org/10.3748/wjg.v17.i5.547.

[35] K.W. Moore, R.D.W. Malefyt, R.L. Coffman, et al., Interleukin-10 and the interleukin-10 receptor, Annual Review of Immunology 19 (2001) 683–765.

[36] K.J. Jung, G.W. Lee, C.H. Park, et al., Mesenchymal Stem Cells Decrease Oxidative Stress in the Bowels of Interleukin-10 Knockout Mice, Gut and Liver 14(1) (2020) 100–107. https://doi.org/10.5009/gnl18438.

[37] A.E. Shin, H.J. Good, Y. Tesfagiorgis, et al., F4/80(+)Ly6C(high) Macrophages Lead to Cell Plasticity and Cancer Initiation in Colitis, Gastroenterology 164(4) (2023) 593–609. https://doi.org/10.1053/j.gastro.2023.01.002.

[38] G.R. Jones, C.C. Bain, T.M. Fenton, et al., Dynamics of Colon Monocyte and Macrophage Activation During Colitis, Frontiers in Immunology 9 (2018) 2764. https://doi.org/10.3389/fimmu.2018.02764.

[39] M.C. Leal, J. Däbritz, Immunoregulatory Role of Myeloid-derived Cells in Inflammatory Bowel Disease, Inflammatory Bowel Diseases 21(12) (2015) 2936–2947. https://doi.org/10.1097/mib.0000000000000511.

[40] C.C., Bain, C.L. Scott, H. Uronen-Hansson, et al., Resident and pro-inflammatory macrophages in the colon represent alternative context-dependent fates of the same Ly6Chi monocyte precursors, Mucosal Immunology 6(3) (2013) 498–510. https://doi.org/10.1038/mi.2012.89.

[41] N. Kamada, T. Hisamatsu, S. Okamoto, et al., Unique CD14+ intestinal macrophages contribute to the pathogenesis of Crohn disease via IL-23/IFN-γ axis, Journal of Clinical Investigation 118 (2008) 2269–2280. https://doi.org/10.1172/jci34610.

[42] L. Peng, X. Gao, L. Nie, et al., Astragalin Attenuates Dextran Sulfate Sodium (DSS)-Induced Acute Experimental Colitis by Alleviating Gut Microbiota Dysbiosis and Inhibiting NF-κB Activation in Mice, Frontiers in Immunology 11 (2020) 2058. https://doi.org/10.3389/fimmu.2020.02058.

[43] J. Wu, Z. Wei, P. Cheng, et al., Rhein modulates host purine metabolism in intestine through gut microbiota and ameliorates experimental colitis, Theranostics 10(23) (2020) 10665–10679. https://doi.org/10.7150/thno.43528.

[44] S. Fernández-Tomé, B. Hernández-Ledesma, M. Chaparro, et al., Role of food proteins and bioactive peptides in inflammatory bowel disease, Trends in Food Science & Technology 88 (2019) 194–206. https://doi.org/10.1016/j.tifs.2019.03.017.

[45] J. Yang, G. Pei, X. Sun, et al., RhoB affects colitis through modulating cell signaling and intestinal microbiome, Microbiome 10 (2022) 149. https://doi.org/10.1186/s40168-022-01347-3.

[46] X. Wang, Q. Luo, J. Yang, et al., Clinacanthus nutans restores the intestinal barrier in UC via regulatings oxidative stress to suppress the occurrence of ferroptosis, Journal of Functional Foods 129 (2025) 106863. https://doi.org/10.1016/j.jff.2025.106863.

[47] T. Kucharzik, S.V. Walsh, J. Chen, et al., Neutrophil Transmigration in Inflammatory Bowel Disease Is Associated with Differential Expression of Epithelial Intercellular Junction Proteins, The American Journal of Pathology 159(6) (2001) 2001–2009. https://doi.org/10.1016/s0002-9440(10)63051-9.

[48] H.X. Guo, Z.H. Ji, B.B. Wang, et al., Walnut peptide ameliorates DSS-induced colitis in mice by inhibiting inflammation and modulating gut microbiota, Journal of Functional Foods 119 (2024) 106344. https://doi.org/10.1016/j.jff.2024.106344.

[49] M.J. Ostaff, E.F. Stange, J. Wehkamp, Antimicrobial peptides and gut microbiota in homeostasis and pathology, EMBO Molecular Medicine 5(10) (2013) 1465–1483. https://doi.org/10.1002/emmm.201201773.

[50] R.A. Ratsimandresey, M. Indramohan, A. Dorfleutner, et al., The AIM2 inflammasome is a central regulator of intestinal homeostasis through the IL-18/IL-22/STAT3 pathway, Cellular & Molecular Immunology 14 (2016) 127–142. https://doi.org/10.1038/cmi.2016.35.

[51] X. Qin, Z. Liu, K. Nong, et al., Porcine-derived antimicrobial peptide PR39 alleviates DSS-induced colitis via the NF-κB/MAPK pathway, International Immunopharmacology 127 (2024) 111385. https://doi.org/10.1016/j.intimp.2023.111385.

[52] X. Ding, H. Yu, S. Qiao, Lasso Peptide Microcin J25 Effectively Enhances Gut Barrier Function and Modulates Inflammatory Response in an Enterotoxigenic Escherichia coli-Challenged Mouse Model, International Journal of Molecular Sciences 21 (2020) 6500. https://doi.org/10.3390/ijms21186500.

[53] X. Liu, C.S. Zhang, C. Lu, et al., A conserved motif in JNK/p38-specific MAPK phosphatases as a determinant for JNK1 recognition and inactivation, Nature Communications 7 (2016) 10879. https://doi.org/10.1038/ncomms10879.

[54] K.A. Gallo, G.L. Johnson, Mixed-lineage kinase control of JNK and p38 MAPK pathways, Nature Reviews Molecular Cell Biology 3 (2002) 663–672. https://doi.org/10.1038/nrm906.

[55] C. Qu, C. Liang, T. Liu, et al., Green tea peptides ameliorate diabetic nephropathy by inhibiting the TGF-β/Smad signaling pathway in mice, Food & Function 13(6) (2022) 3258–3270. https://doi.org/10.1039/d1fo03615g.

[56] T. Saisavoey, P. Sangtanoo, C. Chanchao, et al., Identification of novel anti-inflammatory peptides from bee pollen (*Apis mellifera*) hydrolysate in lipopolysaccharide-stimulated RAW264.7 macrophages, Journal of Apicultural Research 60(2) (2020) 280–289. https://doi.org/10.1080/00218839.2020.1745434.

[57] S. Guha, K. Majumder, Tryptophan end-tagging for promoted lipopolysaccharide interactions and anti-inflammatory effects, Scientific Reports 7(1) (2017) 212. https://doi.org/10.1038/s41598-017-00188-7.

[58] Y. Zhai, X. Shen, R. O'Connell, et al., Cutting Edge: TLR4 Activation Mediates Liver Ischemia/Reperfusion Inflammatory Response via IFN Regulatory Factor 3-Dependent MyD88-Independent Pathway, The Journal of Immunology 173(12) (2004) 7115–7119. https://doi.org/10.4049/jimmunol.173.12.7115.

[59] M. Abdelnaser, M.E. Attya, M.A. El-Rehany, et al., Clemastine mitigates sepsis-induced acute kidney injury in rats; the role of α-Klotho/TLR-4/MYD-88/NF-κB/ Caspase-3/ p-P38 MAPK signaling pathways, Archives of Biochemistry and Biophysics 763 (2025) 110229. https://doi.org/10.1016/j.abb.2024.110229.

[60] X. Wang, Y. Gao, L. Wang, et al., Troxerutin improves dextran sulfate sodium-induced ulcerative colitis in mice, Journal of Agricultural and Food Chemistry 69 (2021) 2729–2744. https://doi.org/10.1021/acs.jafc.0c06755.

[61] B. Mahieu, E.M. Qannari, B. Jaillais, Extension and significance testing of Variable Importance in Projection (VIP) indices in Partial Least Squares regression and Principal Components Analysis, Chemometrics and Intelligent Laboratory Systems 242 (2023) 104986. https://doi.org/10.1016/j.chemolab.2023.104986.

[62] E.S. Ali, I. Ben-Sahra, Regulation of nucleotide metabolism in cancers and immune disorders, Trends in Cell Biology 33(11) (2023) 950–966. https://doi.org/10.1016/j.tcb.2023.03.003.

[63] W. Dermauw, T. Van Leeuwen, The ABC gene family in arthropods: Comparative genomics and role in insecticide transport and resistance, Insect Biochemistry and Molecular Biology 45 (2014) 89–110. https://doi.org/10.1016/j.ibmb.2013.11.001.

[64] C.B. Jeong, H.S. Kim, H.M. Kang, et al., ATP-binding cassette (ABC) proteins in aquatic invertebrates: Evolutionary significance and application in marine ecotoxicology, Aquatic Toxicology 185 (2017) 29–39. https://doi.org/10.1016/j.aquatox.2017.01.013.

[65] Z. Wang, F. Tian, L. Cai, et al., Identification of candidate ATP-binding cassette transporter gene family members in *Diaphorina citri* (Hemiptera: Psyllidae) via adult tissues transcriptome analysis, Scientific Reports 9 (2019) 15842. https://doi.org/10.1038/s41598-019-52402-3.

[66] M. Dean, A. Rzhetsky, R. Allikmets, The Human ATP-Binding Cassette (ABC) Transporter Superfamily, Genome Research 11 (2001) 1156–1166. https://doi.org/10.1101/gr.184901.

[67] H. Arora, S.M. Wilcox, L. A. Johnson, et al., The ATP-Binding Cassette Gene ABCF1 Functions as an E2 Ubiquitin-Conjugating Enzyme Controlling Macrophage Polarization to Dampen Lethal Septic Shock, Immunity 50 (2019) 418–431. https://doi.org/10.1016/j.immuni.2019.01.014.

[68] Z. Wang, Q. Shi, Y. Feng, et al., Targeted screening of an anti-inflammatory polypeptide from Rhopilema esculentum Kishinouye cnidoblasts and elucidation of its mechanism in alleviating ulcerative colitis based on an analysis of the gut microbiota and metabolites, Food Science and Human Wellness 13 (2024) 1336–1347. https://doi.org/10.26599/fshw.2022.9250112.

[69] R. Rupprecht, F. Holsboer, Neuroactive steroids: mechanisms of action and neuropsychopharmacological perspectives, Trends Neurosci 22 (1999) 410–416. https://doi.org/10.1016/S0166-2236(99)01399-5.

[70] R.H. PURDY, A.L. MORROW, J. PERRY H. MOORE, et al., Stress-induced elevations of y-aminobutyric acid type A receptor-active steroids in the rat brain, Proceedings of the National Academy of Sciences of the United States of America 88 (1991) 4553–4557. https://doi.org/10.1073/pnas.88.10.4553.

[71] M.A. Rogawski, D.S. Reddy, Neurosteroids and infantile spasms: The deoxycorticosterone hypothesis, International Review of Neurobiology 49 (2002) 199–219. https://doi.org/10.1016/s0074-7742(02)49014-9.

[72] P. Li, G. Chen, J. Zhang, et al., Live Lactobacillus acidophilus alleviates ulcerative colitis via the SCFAs/mitophagy/NLRP3 inflammasome axis, Food & Function 13 (2022) 2985–2997. https://doi.org/10.1039/d1fo03360c.

[73] I. Domínguez-López, C. Arancibia-Riveros, R. Casas, et al., Changes in plasma total saturated fatty acids and palmitic acid are related to pro-inflammatory molecule IL-6 concentrations after nutritional intervention for one year, Biomedicine & Pharmacotherapy 150 (2022) 113028. https://doi.org/10.1016/j.biopha.2022.113028.

[74] C.E. Annevelink, P.A. Sapp, K.S. Petersen, et al., Diet-derived and diet-related endogenously produced palmitic acid: Effects on metabolic regulation and cardiovascular disease risk, Journal of Clinical Lipidology 17 (2023) 577–586. https://doi.org/10.1016/j.jacl.2023.07.005.

[75] Y. Mizushina, N. Takahashi, L. Hanashima, et al., Lucidenic Acid O and Lactone, New Terpene Inhibitors of Eukaryotic DNA Polymerases from a Basidiomycete, Ganoderma lucidum, Bioorganic & Medicinal Chemistry 7 (1999) 2047–2052. https://doi.org/10.1016/S0968-0896(99)00121-2.

[76] C. Kreiss, W. Schwizer, J. Borovicka, et al., Effect of lintitript, a new CCK-A receptor antagonist, on gastric emptying of a solid-liquid meal in humans, Regulatory Peptides 74 (1998) 143–149. https://doi.org/10.1016/S0167-0115(98)00035-4.

[77] R.D. Spence, R.R. Voskuhl, Neuroprotective effects of estrogens and androgens in CNS inflammation and neurodegeneration, Frontiers in Neuroendocrinology 33 (2012) 105–115. https://doi.org/10.1016/j.yfrne.2011.12.001.

[78] K.Y., Yang, C.R. Wu, M.Z., Zheng, et al., Physapubescin I from husk tomato suppresses SW1990 cancer cell growth by targeting kidney-type glutaminase, Bioorganic Chemistry 92 (2019) 103186. https://doi.org/10.1016/j.bioorg.2019.103186.

[79] D.A. York, L. Singer, J. Oliver, et al., The detrimental effect of simmondsin on food intake and body weight of rats, Industrial Crops and Products 12 (2000) 183–192. https://doi.org/10.1016/S0926-6690(00)00070-4.

[80] R.R. Voskuhl, H. Wang, T.C.J. Wu, et al., Estriol combined with glatiramer acetate for women with relapsing-remitting multiple sclerosis: a randomised, placebo-controlled, phase 2 trial, The Lancet Neurology 15(1) (2016) 35–46. https://doi.org/10.1016/s1474-4422(15)00322-1.

[81] I. Zahoor, T.A. Mir, T.A. Ganaie, et al., Antidiabetic potential from selected Himalayan underutilized herbs: a review, Food and Humanity 2 (2024) 100297. https://doi.org/10.1016/j.foohum.2024.100297.

[82] P. Song, Q. Jiang, X. Wu, et al., Palmitic acid and palmitoylation in cancer: Understanding, insights, and challenges, The Innovation 6(8) (2025) 100918. https://doi.org/10.1016/j.xinn.2025.100918.

[83] F. Xu, K. Hu, A. Mohsin, et al., Recent advances in the biosynthesis and production optimization of gentamicin: A critical review, Synthetic and Systems Biotechnology 10(1) (2025) 247–261. https://doi.org/10.1016/j.synbio.2024.11.003.